C.P. No. 687

MINISTRY OF AVIATION

AERONAUTICAL RESEARCH COUNCIL

CURRENT PAPERS

The Mixing with Ambient Air of a Cold Airstream in a Centrifugal Field

By

B.S. Stratford, Z.M. Jawor and G.T. Golesworthy

The mixing with ambient air of a cold airstream
in a centrifugal field
- By -
B. S. Stratford, Z. M. Jawor and G. T. Golesworthy

June, 1962

SUMMARY

Tests have been made to compare the rate of mixing with ambient air of a single-sided cold air jet when flowing over straight and curved surfaces. The rate of mixing, defined as the rate of entrainment of ambient air into the stream, was determined in two ways: from direct measurement of the increase of mass flow inside the jet and from the entrainment velocity derived from measurements of the static pressure close to the jet boundary.

The experimental results, though showing considerable scatter, lend confirmation to earlier deductions that a centrifugal field increases the mixing rate. A typical increase in mixing rate is 50%.

A theoretical analysis, developed from mixing length concepts, shows that the increase in mixing rate is approximately proportional to the strength of the centrifugal field. The increase results from the eddies of air from the higher momentum stream being centrifuged through surrounding air of lower momentum.

The experimental results are broadly in agreement with the theory, as well as with previous experimental work.

CONTENTS

- -

ILLUSTRATIONS

ILLUSTRATIONS (cont'd)

1. Introduction

Investigations at the N.G.T.E.[1,2,3] have suggested that the centrifugal field associated with a curved flow path increases the mixing rate between adjacent hot and cold gas streams. Caille[4], and more recently Bradshaw & Gee[5], have obtained experimental results for the mixing of a single-sided cold jet in still air and they, too, find an increase in the mixing rate as a result of a centrifugal field. Such results could have application to certain regions of an aircraft propulsion system, where mixing rate is an important parameter in determining length and weight.

As a first step towards obtaining a better understanding of the possible flow in an engine it was decided to try to simplify the problem. Consequently the mixing of the cold jet in still air was selected for study in preference to mixing between hot and cold streams, on the assumption that the basic effect of the centrifugal field would be the same in both types of flow. The results from such a study should also be applicable to the "Coanda" type of flow obtained on an aircraft wing having either injection boundary layer control or a jet flap. A theory for the cold jet was therefore developed from mixing length concepts for turbulent flow and a series of tests conducted to give a comparison of the rate of mixing for models of different configurations.

Considerable difficulties were experienced with the test models partly due to sensitivity of the airflow to upstream conditions. In the original build standard precautions had been taken, but these proved insufficient and special precautions were found to be necessary. Some of the difficulties were due to the small aspect ratio, which resulted from the use of parts of an existing rig.

There is a resemblance between the present type of flow and that in a gravitational field with density stratification. The latter flow has been considered by Stokes, Taylor[6], Goldstein[7], Drazin[8] and others, their primary concern being the stability of the laminar regime. It has also been considered by Ellison & Turner[9] and others for turbulent flow. However, in the gravitational field it is essentially the density gradient which affects the stability and the rate of mixing. In the centrifugal field, on the other hand, it would seem to be primarily the gradient of total pressure which is important, although the density gradient may have an indirect effect by altering the local total pressure. A further difference in the problems is that the gravitational fields considered have all had a stabilising gradient, whereas the present gradient is destabilising. In addition, the present treatment includes the tentative theoretical approach for the turbulent flow.

2. Theory

In mixing length theory a portion of the fluid - loosely referred to as an eddy - is supposed to have a transverse movement, L, due to turbulence. The eddy carries with it its initial properties such as longitudinal velocity and these are imparted to the surrounding flow at the end of the transverse movement. Standard analysis for the resulting momentum exchange then shows that the various mixing rates of the jet, for example the rate of spread of the cold jet in still air or the rate of entrainment of the surrounding air into the jet, are proportional to L^2. The present analysis aims at finding the increase in the transverse movement L resulting from the differential centrifugal action on the eddy; the increase in rate of spread, etc., is then readily deduced. While the derivation of the theory holds for when there is an external flow, the simplest configuration is that with a single jet in still air; the jet is two-dimensional and one-sided, the formation with and without the centrifugal field being illustrated in Figure 1.

For pure circular motion, as in a free vortex, there is a radial, or transverse, pressure gradient given by

$$\partial p/\partial y = \rho u^2 \kappa \qquad \qquad \dots (1)$$

where p is the static pressure, u is the flow velocity and ρ the density; κ is the flow path curvature and y the distance measured perpendicular to the flow. The curvature of the flow is therefore related to the transverse pressure gradient by

$$\kappa = (\partial p/\partial y)/\rho u^2 \qquad \qquad \dots (2)$$

Equation (2) is assumed to be applicable in the present configuration, the various quantities being taken as mean values at any point.

Consider now the mixing region between two streams having velocities U_1 and U_2 as in Figure 2, the stream U_1 of greater velocity being nearer the wall (which, in the case of the curved wall, is shown developed in this Figure). The velocity of an outward moving eddy exceeds that of the surrounding flow as it has come from a region of higher velocity; the difference is indicated by δu in Figure 2. However, its density is the same as that of the surrounding fluid, and it is in the same pressure gradient. Consequently, from Equation (2), the curvature of its flow path will be less than that of the surrounding fluid. The higher velocity eddy is therefore being differentially centrifuged through the fluid. It is an estimate of this effect which is required.

Suppose that the mean flow path curvature for the eddy is κ_e, suffix e denoting the eddy, and suppose that the longitudinal distance travelled by the eddy during its transverse movement is d. Then, by differential geometry, or, more crudely, from Figure 3, the difference in flow path curvatures will give the eddy a transverse movement relative to the rest of the fluid - additional to the basic transverse movement L - of

$$Y - Y_e = \tfrac{1}{2}d^2\kappa(1 - \kappa_e/\kappa) \qquad \qquad \dots (3)$$

The derivation of Equation (3) has ignored the inclined direction of the path of the eddy during its transverse motion as the effects of this inclination appear to cancel when a mean is taken over both the outward and the inward moving eddies. From Equations (2) and (3),

$$Y - Y_e = \tfrac{1}{2}d^2\kappa(1 - (u/u_e)^2) \qquad \qquad \dots (4)$$

u and u_e being the longitudinal velocities of the surrounding flow and of the eddy, respectively, at the middle of the transverse movement. Putting

$$u_e = u + \delta u \qquad \qquad \dots (5)$$

where $\delta u/u$ is supposed small, Equation (4) gives

$$Y - Y_e \doteqdot d^2 \kappa \delta u/u \qquad \qquad \dots (6)$$

If the increase in the original transverse movement L is $L\varepsilon$,

$$L\varepsilon = Y - Y_e$$

and, from Equation (6),

$$\varepsilon = d^2 \kappa \delta u / L u \qquad \dots\ (7)$$

From Figure 2 the value of δu at the middle of the movement is

$$\delta u = \tfrac{1}{2} L (1 + \varepsilon)(-\partial u/\partial y) \qquad \dots\ (8)$$

Hence, from Equation (7), ε is given by

$$\varepsilon/(1 + \varepsilon) = (d^2 \kappa / 2u)(-\partial u / \partial y) \qquad \dots\ (9)$$

It follows that if the ratio of the mixing length in curved flow to that in straight flow is denoted $\overline{L}$,

$$\overline{L} = 1 + \varepsilon = 1/\{1 - (d^2 \kappa / 2u)(-\partial u/\partial y)\} \qquad \dots\ (10)$$

It remains only to determine d.

In the mixing between two straight flows the motion of an eddy has a mean inclination, say Θ, to the direction of the surrounding streams, given by

$$\tan \Theta = L/d \qquad \dots\ (11)$$

Also if v' is the mean transverse velocity of the eddy during its movement

$$\tan \Theta = v'/u \qquad \dots\ (12)$$

Hence

$$d = uL/v' \qquad \dots\ (13)$$

Now v' as just defined is the mean transverse component of turbulent velocity during and due to the movement, while the corresponding mean longitudinal component, u', is just $\tfrac{1}{2} L | \partial u/\partial y |$, as for Equation (8). Furthermore, there is experimental evidence that the root mean square turbulent velocity components tend to be about equal in many turbulent flows - for example see Table II of Reference 10 - and so it will be assumed that the present components v' and u' are equal. Hence

$$v' = u' = \tfrac{1}{2} L | \partial u/\partial y | \qquad \dots\ (14)$$

Thus, from Equation (13)

$$d = 2u/| \partial u/\partial y | \qquad \dots\ (15)$$

The further assumption is now made that the eddy moves transversely, before being brought to relative rest by the surrounding fluid, for the same length of time in curved flow as in straight flow; consequently the length d is also the same in the two flows. Substitution into Equation (10) then gives

$$\bar{L} = 1/\{1 - 2u\kappa/(-\partial u/\partial y)\} \qquad \dots \dots (16)$$

Equation (16) indicates the increase in the transverse movement at any position on the velocity profile.

In order to find the effect for the whole mixing region a mean value is required for the quantity $u/(\partial u/\partial y)$ across the velocity profile. Since the mixing in the "tails" of the velocity profile shown in Figure 2 is probably not important the profile is assumed for the present purpose to be equivalent to a linear profile of width $2b/3$, the required mean value being taken as

$$\{u/(-\partial u/\partial y)\}_{mean} = \tfrac{1}{2}(U_1 + U_2)/\{(U_1 - U_2)/\tfrac{2}{3}b\} \qquad \dots \dots (17)$$

$$= \tfrac{1}{3}b(U_1 + U_2)/(U_1 - U_2)$$

The value of $\bar{L}$ for the whole mixing region then becomes

$$\bar{L} = 1/\{1 - \tfrac{2}{3}(b/r)(U_1 + U_2)/(U_1 - U_2)\} \quad \dots (18)$$

where r is the radius of curvature of the mean flow path in the mixing region. For a jet in still air $U_2 = 0$ and

$$\bar{L} = 1/(1 - \tfrac{2}{3}b/r) \qquad \dots \dots (19a)$$

$$= 1 + \tfrac{2}{3}b/r + \tfrac{4}{9}(b/r)^2 + \dots \qquad \dots \dots (19b)$$

Because of the crudity of the assumptions - in particular the neglect of the drag forces on the eddy until the end of the movement - Equation (19a) should really contain a coefficient of ignorance. As an example of the result in its present form Equation (19a) gives that for, $b/r = \tfrac{1}{4}$, $\bar{L} = 1.20$ and hence the increase in rate of spread of the jet would be 44%.

The preceding analysis examines the effect of the centrifugal field on the mixing rate at the local chordwise station. Now, as pointed out by Caille[4], an increase in mixing rate at one chordwise station would cause an increase turbulence level that would be expected to persist for some distance downstream, so that the subsequent mixing rate would also be increased. No analysis, however, has been attempted for this effect.

3. Experimental Work

3.1 Test apparatus

The apparatus, illustrated in Figures 4 to 8 consisted of a circular duct of 4 in. diameter leading to a $6\tfrac{1}{2}$ in. × 4 in. rectangular section and a two-dimensional contraction of area ratio 4.65/1; the latter formed a nozzle 0.86 in. deep and $6\tfrac{1}{2}$ in. span to which various perspex test sections were attached. Initially, in order to obtain a uniform velocity distribution at the nozzle outlet, two wire gauzes of 30 mesh, 32 s.w.g.

(nominally two dynamic heads loss) and two honeycombs were fitted in the rectangular section upstream of the contraction. During preliminary testing it was found necessary to add a third gauze and a third honeycomb, these being placed in the circular ducting. Trip wires of 0.025 in. diameter were placed on the two main surfaces of the contraction, $1\frac{3}{8}$ in. upstream from the nozzle outlet for the profiled surface and $1\frac{5}{8}$ in. for the flat surface, in an attempt to fix the transition point of the boundary layer and thus to render the flow less sensitive to external conditions. Air for the rig was supplied by a Lysholm compressor, capable of operation at 2.7/1 pressure ratio.

The perspex models, or test sections, consisted essentially of either straight or convex test surfaces. Side walls having a faired entry were fitted in order to reduce the outside interference and to obtain uniform spanwise entrainment of the surrounding air. Five different models were used.

Configuration A - 24 in. straight model

Configuration B - 4 in. radius model

Configuration C - 6 in. radius model

Configuration D - 6 in. straight and 4 in. radius model

Configuration E - 6 in. straight and 6 in. radius model

Cross-sectional sketches are shown in Figure 5.

3.2 Instrumentation

3.2.1 Measurements inside the jet stream

The test surfaces of the models were drilled for static pressure tappings and to permit traversing for total and static pressures. The total pressure probe, made of $1\frac{1}{2}$ mm hypodermic tubing with a 1 in. long head, had its entry lip internally bevelled in an endeavour to reduce sensitivity to incidence. The static pressure was measured with a probe having a 1.9 in. head and a nose cone of $10°$ included angle. Four 0.010 in. diameter holes equally spaced circumferentially 1 in. from the stem permitted the static and total pressures to be measured at the same positions. A depth micrometer traversing head, which could be positioned easily at almost any place on the test surface, allowed either probe to be traversed in increments of thousandths of an inch. Figure 6 shows the traversing head and total pressure probe fitted on the 24 in. straight model. The pressures were recorded on a single limb water manometer.

3.2.2 Measurements outside the jet

The static pressure outside the jet was measured by a flat stream-lined probe attached to a $\frac{1}{4}$ in. diameter shaft. The probe shape was chosen to offer minimum resistance to the entrained air parallel to the shaft while not being over-sensitive to eddies of air from the main jet. A 0.040 in. diameter hole drilled on each side of the probe transmitted the static pressure to a Betz manometer capable of an accuracy of 0.05 mm of water. In conjunction with the measurement of the static pressure, a smoke generator[11] and streamlined probe (see Figures 7 and 8) supplied a thin filament of paraffin vapour for tracing the streamlines of the entrained air. The secondary flow effects and the boundary of the jet were investigated by tufts.

3.3 Principal tests and analysis

The experimental investigation proved to be more difficult than expected. Initially the analysis was based upon the divergence angle of the jet, or more strictly, upon db/dx, where b represents the width of the mixing region at a distance x from the nozzle, measured along the mean line of the mixing region. An increase in the value of db/dx for a curved jet as compared with the value for a straight jet should indicate an increase in mixing rate. However, due to the behaviour of the boundary layer, which thickened very rapidly in the pressure rise at the end of the turn in the curved models, it was impossible to differentiate between the increase in db/dx resulting from more rapid mixing and the increase caused by the pressure rise acting upon the boundary layer. Also b was not readily determined accurately as the edge of jet was not well defined. Therefore this method of analysis was abandoned.

The second method of analysis was based upon the rate of increase of mass flow in the jet, i.e., dQ/dx, the mass flow being computed from pitot and static pressure traverses inside the jet stream at mid-span. This type of analysis requires good spanwise uniformity in order that the traverses at the mid-span shall represent the whole flow. Now any slight non-uniformity in the jet at the beginning of the turn tends to be magnified in the destabilising centrifugal field; for example, a slight spanwise variation in thickness would result in a lower static pressure in the thicker parts of the jet than at the thinner, so that secondary flow would occur accentuating the difference in thickness. Considerable difficulties were experienced due to this sensitivity to the upstream conditions. A satisfactory flow was eventually obtained by adding the third gauze and the third honeycomb, by removing a right-angled bend in the supply ducting, by changing to a control valve at 69 diameters upstream from the nozzle outlet in place of one at 39 diameters, and by very careful alignment of the rig and perspex models. The change in the control position resulted in a quieter jet as well as an improved mass flow distribution.

The procedure adopted on each model was to carry out a set of traverses checking the spanwise uniformity of the flow, prior to making the main traverses at mid-span. The traverses for checking spanwise uniformity were made at seven equally spaced positions 19 in. from the nozzle outlet in the case of the 24 in. straight model (configuration A) and at the position corresponding to a 45° angle turn in the other models. The main traverses, i.e., at mid span, were then made at 2 in. intervals on the straight model and at 15° intervals on the curved models, with the exception of models of configuration B and D, where the 75° angle position was omitted due to mechanical difficulties in traversing. The velocity head of the jet at the inlet to the models was kept constant at 13 ± 0.05 in. of water, corresponding to 238 ± 0.5 ft/s.

Figure 9(a) shows three typical pitot traverses at mid-span for the 24 in. straight model. The 2 in. position traverse shows the jet to consist of a mainstream of constant total pressure, together with a mixing zone and a thin boundary layer. The 9 in. and 19 in. traverses show fully developed profiles. In all instances the pressures P_t registered by the pitot tubes are slightly below atmospheric on the very edge of the jet owing to the 90° incidence between the entrained air and the tube.

The boundaries determining the width b of the mixing region were taken arbitrarily to lie where the measured total pressure P_t was atmospheric, and where it was a maximum. For each model the line passing through the middle of the mixing region was established and distances measured along it from the nozzle to each traverse station. Distances along this mean line are appreciably larger than distances measured around the surfaces of the curved models and must, therefore, be used in preference to surface distance when assessing mixing rates. The measured distances x are used in the non-dimensional form x/h, where h, the nozzle height, is a parameter to which all other variables could be related.

The mass flow passing through the jet stream per unit span was obtained at each chordwise station by the integration of the velocity profile derived from the pitot and static traverses, and then plotted against x/h. A typical specimen is shown in Figure 10(a), the mass flow being in the non-dimensional form $\bar{Q} = Q/Q_N$; Q_N is the nominal mass flow per unit span at the nozzle outlet, i.e., $Q_N = \rho U_N h$, $\frac{1}{2}\rho U_N^2$ being the gauge total pressure upstream of the contraction. The gradient of the curve at any point (Figure 10(b)) is

$$\frac{d\bar{Q}}{dx/h} = \frac{dQ}{dx}\frac{h}{\rho U_N h} = \frac{\rho u_{en}}{\rho U_N} = \frac{u_{en}}{U_N}$$

u_{en} being the velocity which the entrained air would require were it to pass normally across the mean mixing line. When the gradient is divided by the velocity ratio U_p/U_N (Figure 11(a)), U_p being the peak velocity at a given chordwise station, it gives the ratio of the entrained to the local peak velocity, u_{en}/U_p (Figure 11(b)). The corresponding results for the 6 in. radius model, configuration C, which has been selected as an example of the curved models, are shown in Figures 12 to 14. It will be seen later (Figure 16) that the curvature effects appear somewhat exaggerated in configuration C.

The velocity ratio u_{en}/U_p, i.e., the ratio of the entrainment velocity to the local peak velocity, may be taken as representative of the mixing rate of each jet. Ordinarily, for a jet in still air, the entrainment to peak velocity ratio is in the region of $1/25$, i.e., 0.04. The present results for the one-sided straight jet are in reasonable agreement with this value, giving $u_{en}/U_p = 0.036$ (Figure 11(b)). On the other hand for the curved jets typical values are 0.05 to 0.06, e.g., see Figure 14(b), thus indicating an increase in mixing rate of the order of 50% as a result of the centrifugal field.

Before making the detailed comparison between the straight and curved flows another feature of the flow requires mention. It will have been noticed from Figure 11(b) that the ratio u_{en}/U_p is initially constant - as for a pure jet in still air - but then decreases with distance along the jet. The decrease is attributed to the damping effect of the end walls on the turbulence when the depth of the mixing region becomes comparable with the span of the model. For example, at $x/h = 16$, where the entrainment velocity ratio has decreased 10%, the depth of the mixing region has increased to about a third of the span. Any given

result for the curved models must therefore be compared with the result for the straight model taken at an equal depth, b, for the mixing region - in order to ensure that the effects of the side walls in damping the turbulence has the same magnitude in both instances. The analysis is also limited to 45° of turn, as the secondary flow in the boundary layer appeared appreciable at greater angles and would cause variation across the span.

The results are shown in comparison with the theory of Section 2 in Figure 15, where the square root of the ratio of the mixing rates in the curved flows to that in the straight flow is plotted against b/R, R being a quantity defined below. Since, in mixing length theory, the mixing rate is proportional to the square of the eddy mixing length L, the ordinate represents L, the ratio of the mixing lengths in the curved and straight flows. The distance R which appears in the abscissa is the nearest practical equivalent to the radius of curvature of the mean mixing line, which in a "Coanda" type flow is difficult to determine accurately. R is actually the distance from the mean mixing line to the centre of curvature of the solid surface. The dashed lines represent the experiment just described. The scatter is large as the results represent a tangent, or differentiation, of the experimental curve of mass flow against distance.

In order to reduce the scatter the local differentiations have been replaced by a mean value for each model; the corresponding results are shown in Figure 16. Agreement with the theory is seen to be quite reasonable; the scatter is still considerable, however, and is probably attributable to the rather difficult circumstances of the mass flow measurement. A suggested range of uncertainty in the experiment is shown.

Because of the difficulties in the analysis based on mass flow a third method of analysis was introduced. This attempted a direct measurement of the entrainment velocity by using a sensitive Betz manometer to measure the static pressure near the edge of the jet. The method should thus be independent of secondary flow within the jet. The jet velocity head was increased to 46 ±0.05 in. of water, equivalent to 448 ±0.25 ft/s, in order to facilitate the measurement. It was found, however, that close to the edge of the jet no reliable readings of static pressure could be obtained. It was therefore decided to measure the static pressure some distance away from the jet, and to deduce the entrainment velocity closer to the jet by tracing streamlines using the smoke generator and probe. The method then comprised the marking of two bands on one of the side walls of the model, the first band a few inches away from the jet boundary and the other as near as possible to the edge of the jet. The band farthest from the jet, i.e., band 'B', was marked in 1 in. intervals and the mid-span static pressure obtained with the special probe at the centre of each interval. The streamlines at mid-span were traced successively from the points marked on band B to the inner band A, where the intersections were marked and measured - care being taken to avoid parallax. The streamlines so obtained were extrapolated to the mean mixing line and, by application of the condition for continuity, the equivalent entrainment velocity at the mean mixing line calculated. A preliminary check on one of the curved models showed that if a third band, C, were placed outside B, the static pressures measured on B and C were in fact consistent with the streamlines traced between B and C and continuity in the flow.

Figure 17 shows the position of the two bands and the paths of streamlines on the 24 in. straight model. The corresponding readings of the Betz manometer, together with the distance measurements, are presented in Figure 18(a) and, when combined with the curve for the velocity ratio U_p/U_N, presented in Figure 11(a), give the ratio of entrained to peak velocity as in Figure 18(b). The corresponding results for one of the curved models, configuration C, are shown in Figures 19 and 20. Comparison between the curved and straight models for the same mixing depth b gave the lines in Figure 15. The scatter is seen to have been improved for configurations B and C but not for D and E. When the average for each model is plotted in Figure 16 it falls quite close to the theoretical line.

The method of analysis just described was applied in the curved models only up to an angle of turn of 75°, as at greater angles difficulties were experienced in determining the edge of the jet and the paths of the streamlines.

Though the results shown in Figure 16 indicate on the whole a reasonable agreement between the two main methods of experimental analysis, the graphs of the velocity ratio u_{en}/U_p show a discrepancy. At the small values of x/h, i.e., close to the nozzle outlet, the results obtained by the two methods agree well, but as x/h increases the values diverge - e.g. compare Figures 11(b) and 18(b) or 14(b) and 20(b). The method based on mass flow tends to give a decrease in the velocity ratio with increase in distance from the nozzle outlet - supposedly for the reason mentioned earlier - whereas the method based on measurement of the external static pressure shows an increase. Some experimental work was carried out to try to determine the reason for the discrepancy, but without success. An additional phenomenon to be noted here is that when the control valve at 39 diameters upstream from the nozzle outlet was used to set the test conditions, instead of the one at 69 diameters as for the main tests, the jet mixing was noisier and about 15% more rapid.

When comparing the velocity ratio u_{en}/U_p between straight and curved flow it is not clear whether the peak velocity U_p should be the actual velocity, i.e., calculated from the total pressure taking into account the depression of the static pressure below atmospheric, or whether it should be an equivalent velocity calculated assuming the static pressure to be equal to atmospheric. Consequently a variation was made on the mass flow method of analysis calculating the peak velocity assuming the static pressure to be atmospheric. The value of L became about 5% higher than before for the same value of the parameter b/R, for all the models.

4. Comparison with previous work

An attempt has been made to analyse the results of Caille[4] and of Bradshaw & Gee[5] for comparison with the present experimental results and theory.

As explained by Bradshaw & Gee, measurements at the edge of the jet were very uncertain. Their own analysis used the parameter $\delta_{0.5}$, i.e., the width of the jet from the wall to the point where the velocity equalled half the local peak velocity, as well as δ_j, the boundary layer thickness. Comparison of their straight walled jet with their Coanda jet gives that the rate of thickening $d(\delta_{0.5} - \delta_j)/dx$ for the curved flow is 1.20 times that for the straight - giving $\bar{L} = 1.10$ and the point plotted in Figure 16 of the present paper. In deducing $d(\delta_{0.5} - \delta_j)/dx$ for the curved flow the distance x has been measured along the mean mixing line, as for the present paper, and the analysis has been confined to the length of curved wall having constant static presure. The agreement with the results of the present paper is satisfactory. It should be pointed out, however, that the boundary layer has an even greater increase in its rate of thickening, $d\delta_j/dx$, than has $\delta_{0.5}$ in Bradshaw and Gee's experiment, and it is not clear how this should affect the interpretation. Amongst other factors the boundar layer can be considered to have a small negative value for b/R, so that $\bar{L}$ would be predicted by the present theory to be slightly less than unity. However the turbulence on one side of the point of peak velocity could well affect the rate of thickening of the flow on the other side, so that no firm conclusions can be drawn. Had the comparison been based on $d\delta_{0.5}/dx$, agreement with the present theory would be almost exact.

Caille's paper is concerned with the general result that the mixing rate is greater in a Coanda flow than in straight flow and quotes little in the way of detailed experimental results or details of apparatus. A value for $\bar{L}$ deduced from Caille's paper is shown in Figure 16, but should be regarded as tentative.

It can be stated that there is qualitative agreement between present results and those previously published, but information is not sufficiently precise to justify a firm conclusion.

5. Conclusions

(1) The theoretical and experimental results lend confirmation to earlier deductions that a centrifugal field increases the mixing rate of a jet in still air. A typical increase in mixing rate is about 50%.

(2) The experimental results, though showing a considerable scatter, gave broad agreement with the theory.

(3) Theory indicates that the increase in the mixing rate is approximately proportional to the ratio b/r, where b represents the width of the mixing region and r the radius of curvature of the mean flow path.

(4) An analysis based upon the divergence angle of the jet was not satisfactory; one difficulty arose in differentiating between the increase in angle due to mixing and that resulting from a pressure rise acting upon the boundary layer, and another in the lack of precision in determining the edge of the jet.

(5) The jet flow was very sensitive to the upstream conditions and, on the present methods of analysis, great care was required in the aerodynamic refinement of the rig. A larger aspect ratio would probably have given more accurate results.

List of Symbols

b total width of the mixing region

d distance travelled by the eddy along the jet, during its transverse movement

h height of the nozzle

L transverse movement of the eddy in straight flow

$L(1 + \varepsilon)$ transverse movement of the eddy in curved flow

$\bar{L}$ ratio of the transverse movement in curved flow to that in straight flow, i.e., $\bar{L} = 1 + \varepsilon$

p static pressure

Q mass flow per unit span

Q_N nominal mass flow per unit span at the nozzle outlet based on the mainstream total pressure and atmospheric static pressure

$\bar{Q}$ relative mass flow, i.e., $\bar{Q} = Q/Q_N$

r radius of curvature of the mean flow path in the mixing region

R radius from the centre of curvature of the test surface to the mean mixing line

u local velocity in the direction of the jet

u_{en} velocity of the surrounding air when being entrained into the jet

u', v' turbulent components of velocity parallel and perpendicular to the direction of the jet, expressed as a mean for the transverse movement, and resulting from the movement; ($u' = \delta u$)

U_N velocity in the mainstream at the nozzle outlet, were the static pressure atmospheric

U_1 or U_p peak velocity of the jet

U_2 velocity of the surrounding flow parallel to the jet

x distance from nozzle outlet along the mean mixing line

y distance measured across the jet

Y   displacement inwards from reference tangent line as a result of the curvature

δu mean velocity difference between the eddy and the surrounding fluid, in the direction of the jet

κ curvature of the flow path

ρ fluid density

θ mean direction of motion of the eddy during its transverse movement, relative to the direction of the stream.

Suffix

e   refers to an eddy

REFERENCES

No.	Author(s)	Title, etc.
1	W. Deacon	Unpublished work at N.G.T.E. 1957.
2	E. L. Hartley	Unpublished work at N.G.T.E. 1958.
3	F. J. Bayley	Unpublished work at N.G.T.E. 1956.
4	C. Caille	The even distribution of air emerging at right angles from a duct. Sulzer Technical Review, No. 1, p. 28, 1956.
5	P. Bradshaw M. T. Gee	Turbulent wall jets with and without an external stream. A.R.C. R. & M. 3252. June, 1960.
6	G. I. Taylor	Effect of variation in density on the stability of superposed streams of fluid. Proc. Roy. Soc. 'A' Vol. 132, p. 499. 1931.
7	S. Goldstein	On the stability of superposed streams of fluids of different densities. Proc. Roy. Soc. 'A' Vol. 132, p. 524. 1931.
8	P. G. Drazin	The stability of a shear layer in an unbounded heterogeneous inviscid fluid. Journal of Fluid Mechanics, Vol. 4, Part 2, pp. 214-224. 1958.
9	T. H. Ellison J. S. Turner	Turbulent entrainment in stratified flows. Journal of Fluid Mechanics, Vol. 6, Part 3, pp. 423-448. 1959.
10	J. C. Laurence	Intensity, scale, and spectra of turbulence in mixing region of free subsonic jet, N.A.C.A. Rpt. 1292. 1956 or as A.R.C. 18,005. November, 1955.
11	P. G. G. O'Neill	A generator constructed in metal for producing small quantities of paraffin smoke. N.P.L. Aero. 340. 1957.

FIG. I
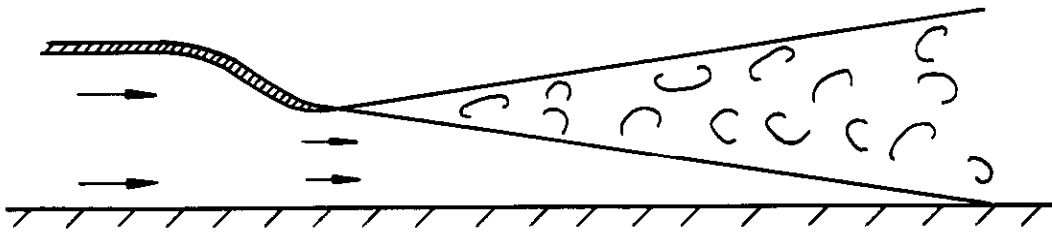
FIG. 1a.   STRAIGHT FLOW — NO CENTRIFUGAL FIELD.
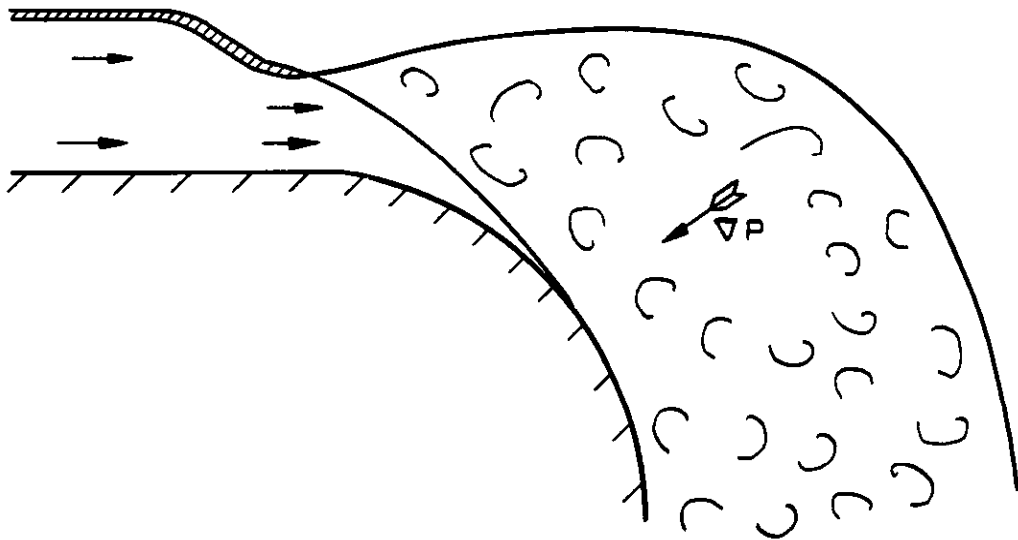
FIG. 1b. CURVED FLOW-WITH CENTRIFUGAL FIELD.

A COLD JET IN STILL · AIR
STRAIGHT AND CURVED FLOW.

FIG. 2

LONGITUDINAL VELOCITY ────▶

(FOR A JET IN STILL AIR $U_2 = 0$)
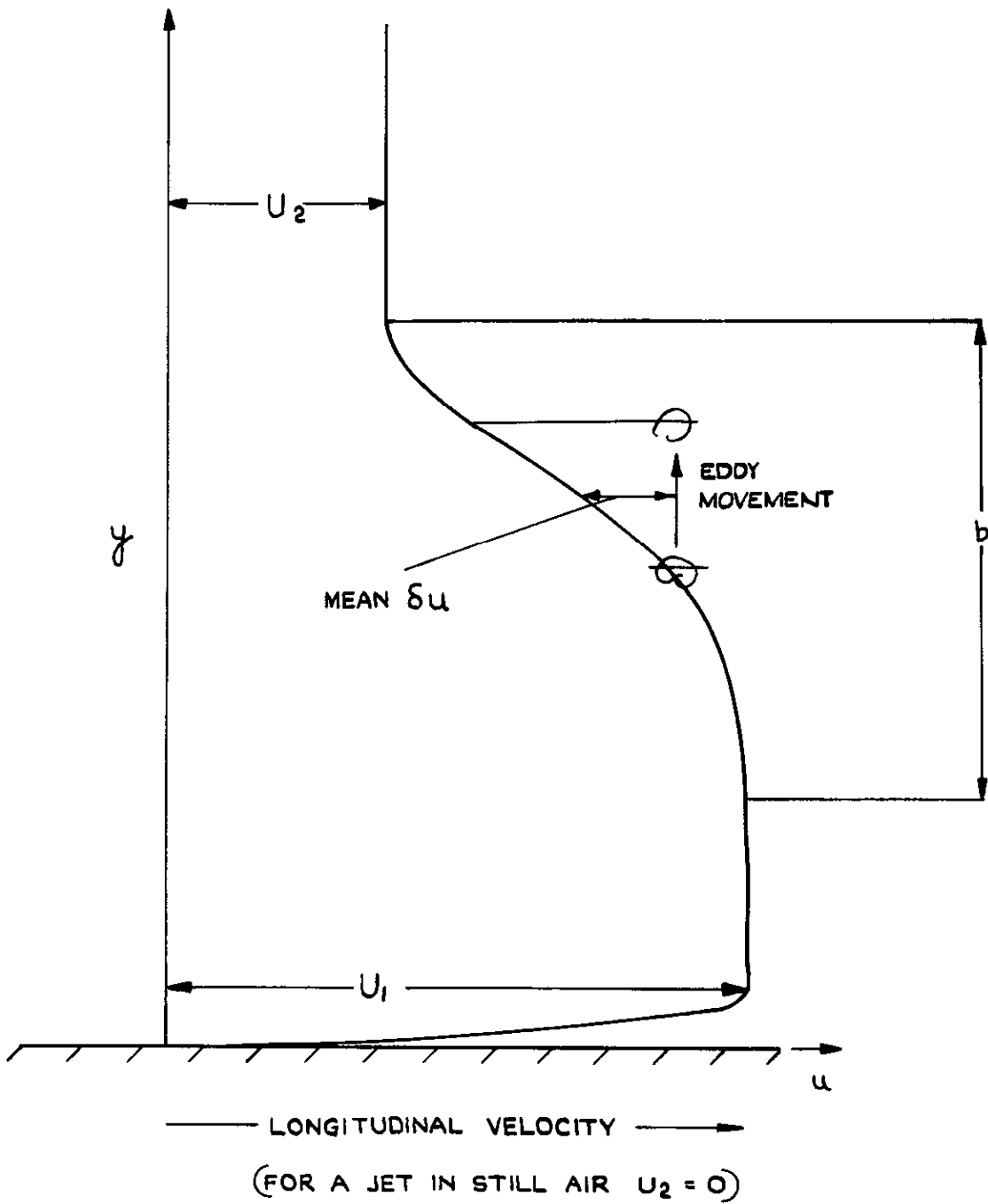
THE VELOCITY PROFILE AND THE TRANSVERSE MOVEMENT OF THE EDDY.

FIG. 3

DISPLACEMENT DUE TO CURVATURE

CURVED FLOW PATH OF MAIN-FLOW
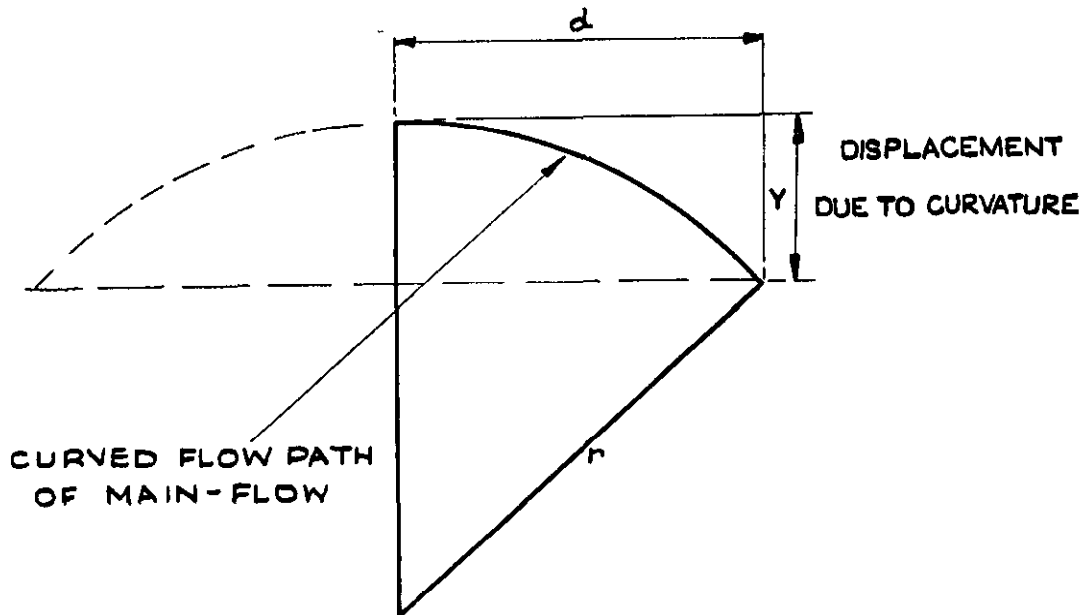
$$d^2 = Y\left(2r - Y\right), \therefore Y \fallingdotseq \frac{d^2}{2r} = \frac{d^2}{2}K$$

FIG.3a. DISPLACEMENT FROM A REFERENCE TANGENT LINE DUE TO CURVATURE.

CURVATURE OF MAIN FLOW PATH

CURVATURE OF EDDY PATH

$$Y - Y_e = \frac{d^2}{2}(K - K_e)$$

THE MAIN TRANSVERSE MOVEMENT L HAS BEEN OMITTED FOR SIMPLICITY.
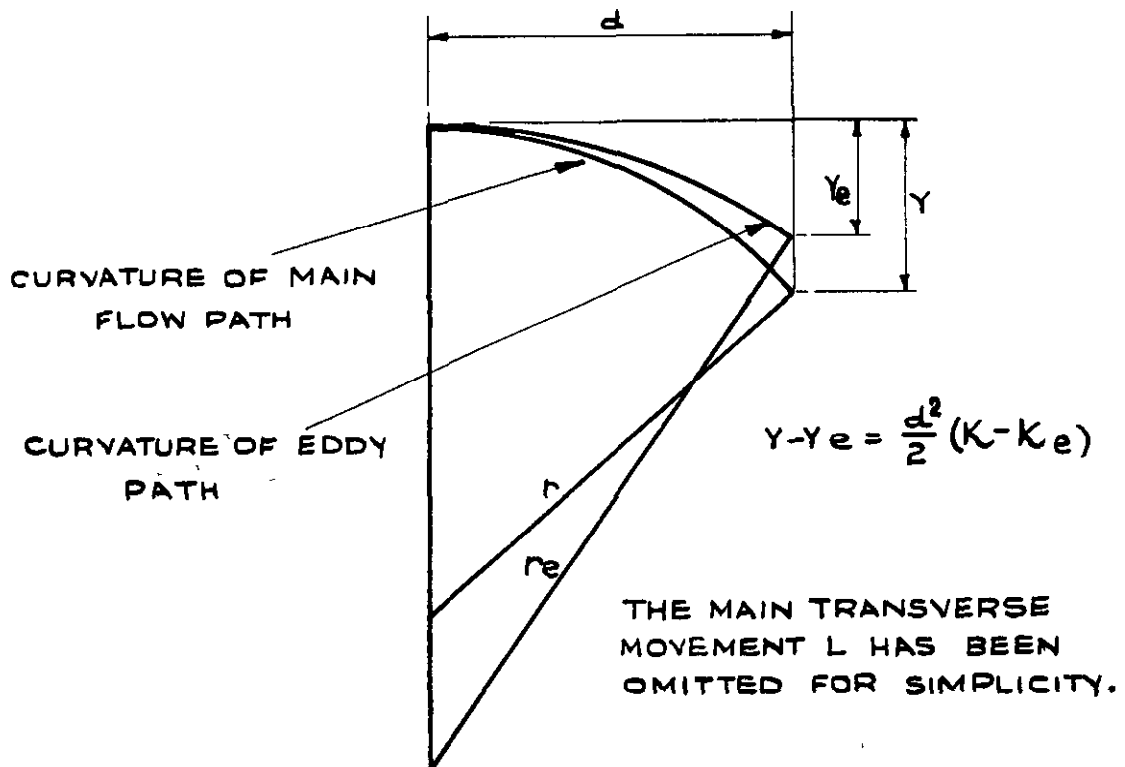
FIG.3b. DIFFERENTIAL DISPLACEMENT RESULTING FROM DIFFERENTIAL CURVATURE OF PATHS.

THE DIFFERENTIAL CENTRIFUGAL MOVEMENT.

FIG. 4

SCALE (INS)

0 2 4 6

SECTION A-A'

FAIRING

TRIP WIRES

STATIC PRESSURE

STATIC PRESSURE

PITOT PRESSURE

GAUZE

A

A'—A'
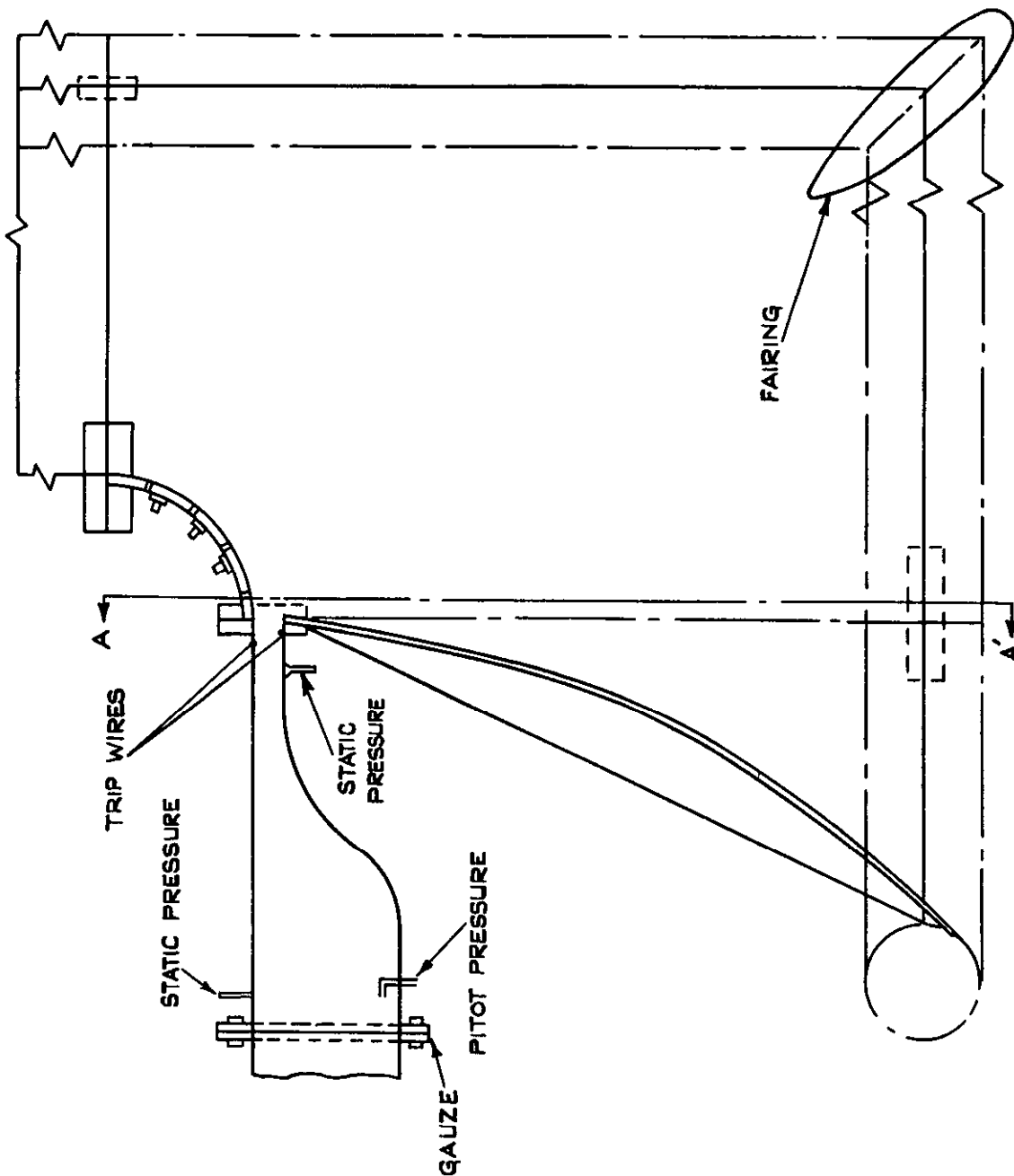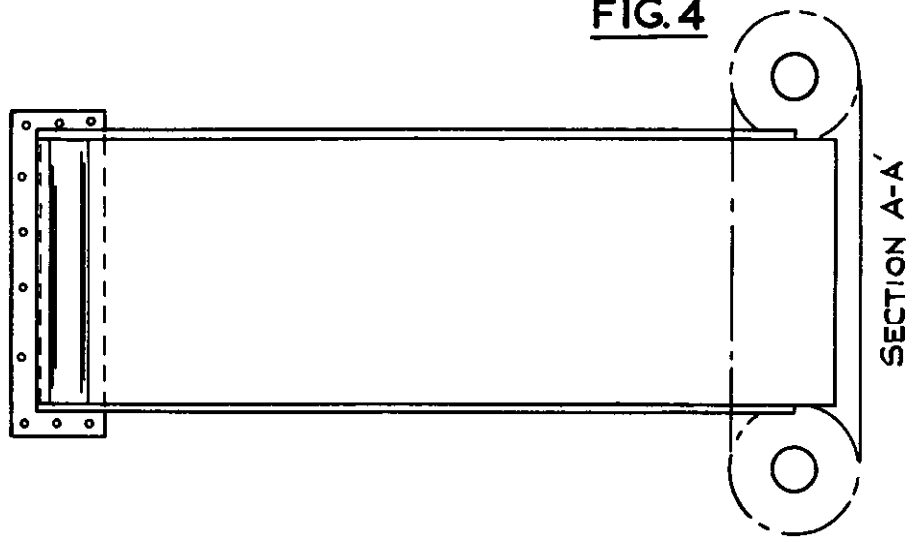
CROSS SECTIONAL SKETCH OF THE RIG
WITH THE 4 IN. RADIUS MODEL.

FIG. 5

NOZZLE EXIT

|← 24 IN →|

CONFIGURATION A.

NOZZLE EXIT

4 IN RAD

24 IN

CONFIGURATION B.

NOZZLE EXIT

6 IN RAD

24 IN

CONFIGURATION C.

NOZZLE EXIT

|← 6 IN →|

4 IN RAD

24 IN.

CONFIGURATION D.

NOZZLE EXIT

|← 6 IN →|

6 IN RAD

24 IN.
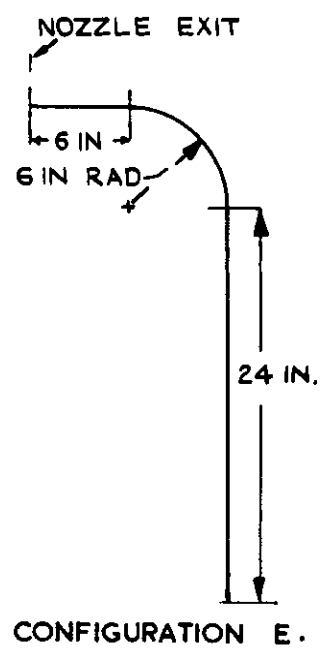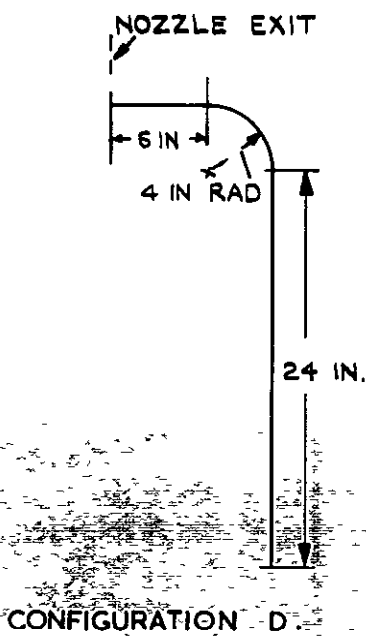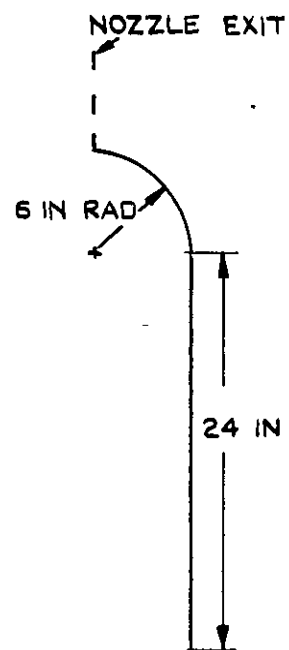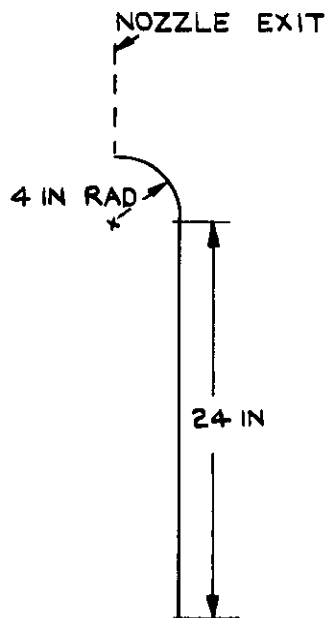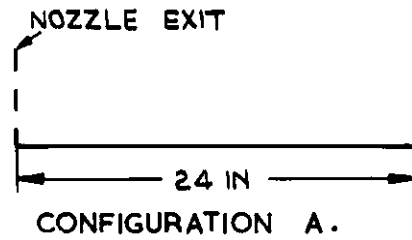
CONFIGURATION E.

CROSS SECTIONAL SKETCHES
OF THE MODELS.

FIG. 6.

TRAVERSER
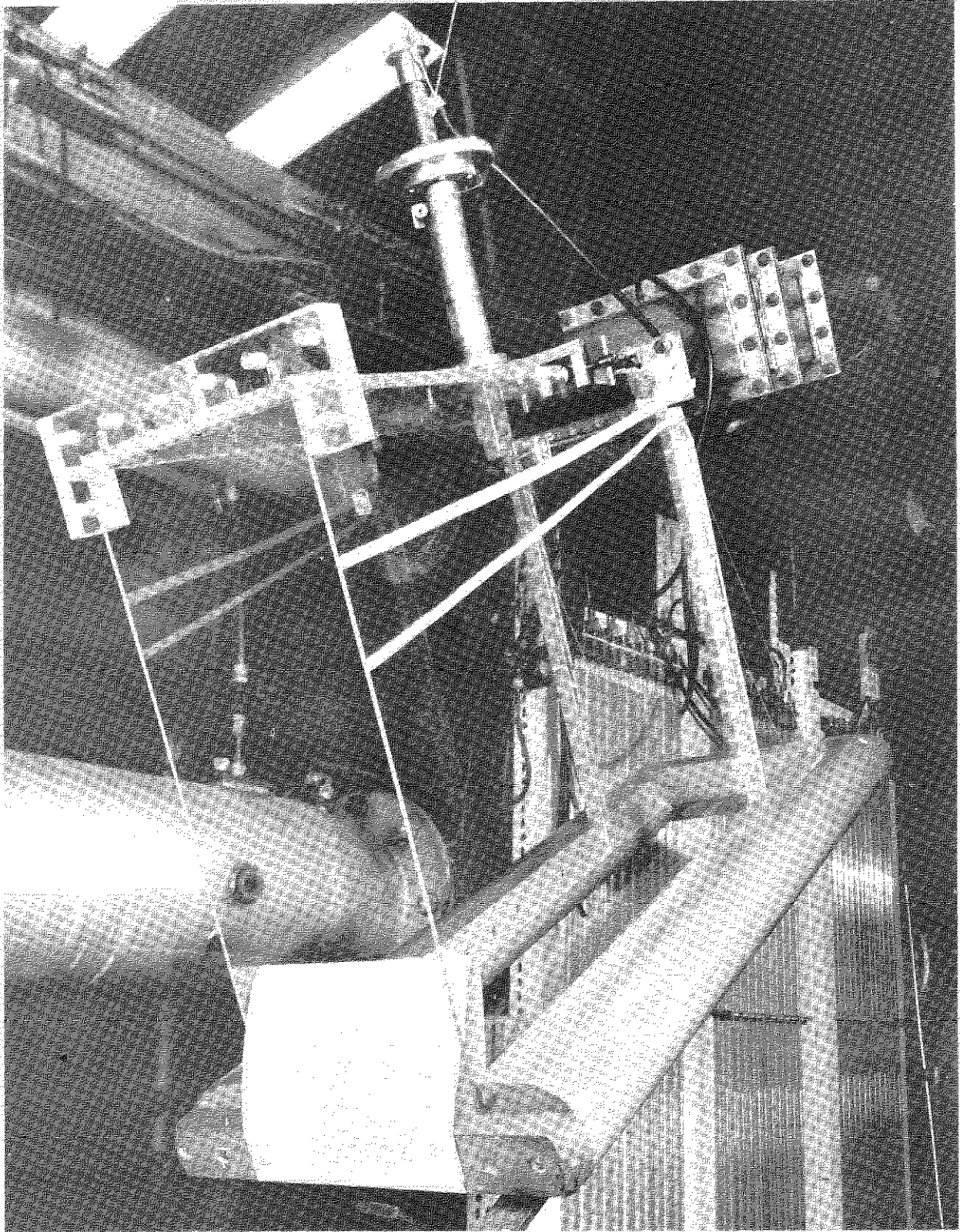
24IN. STRAIGHT MODEL READY FOR
TESTING

FIG. 7.
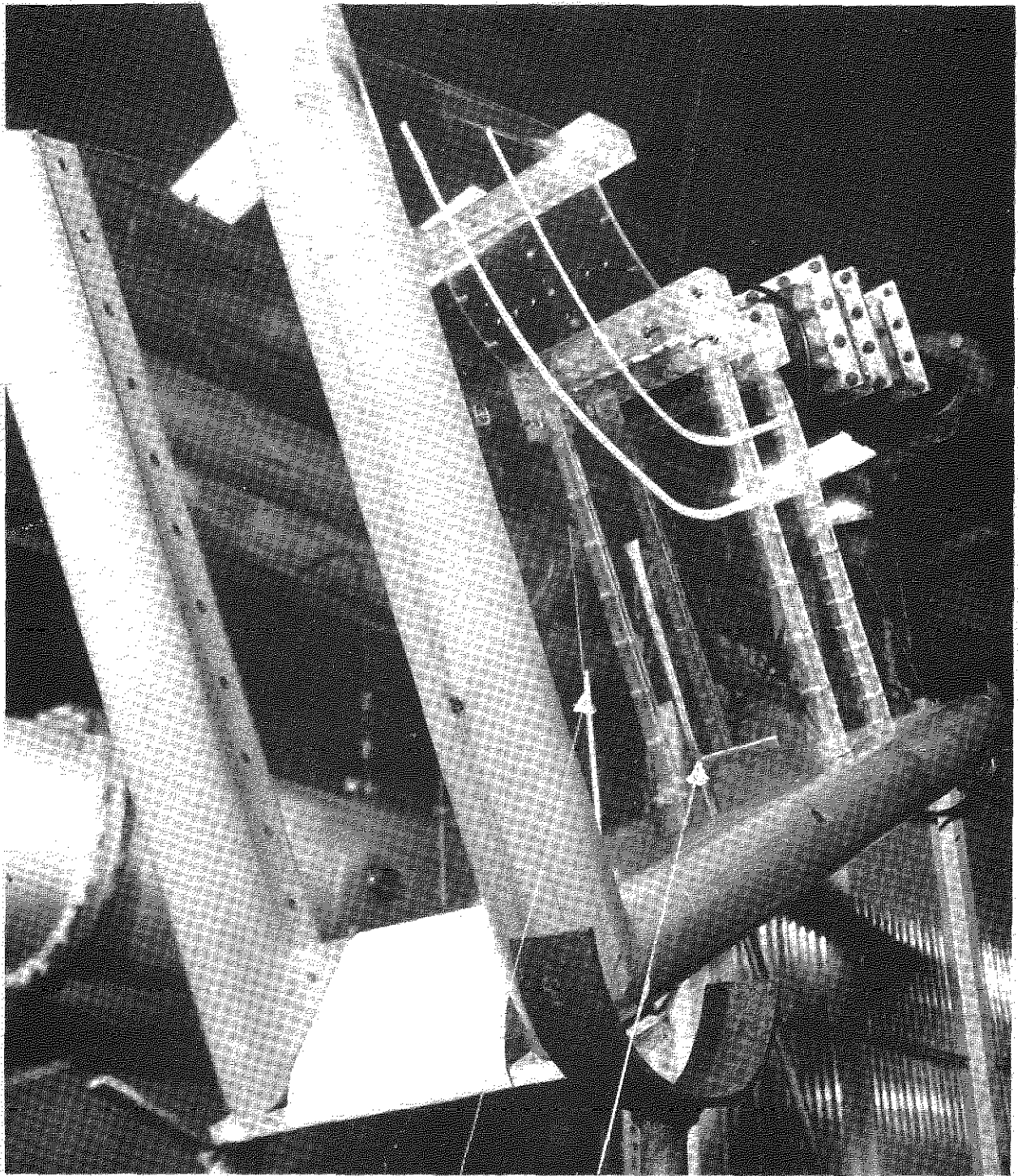
SMOKE PROBE

SPECIAL STATIC PROBE

(NOT USED SIMULTANEOUSLY)

CURVED MODEL CONFIGURATION E WITH
24IN. PORTION REMOVED.

SMOKE PROBE
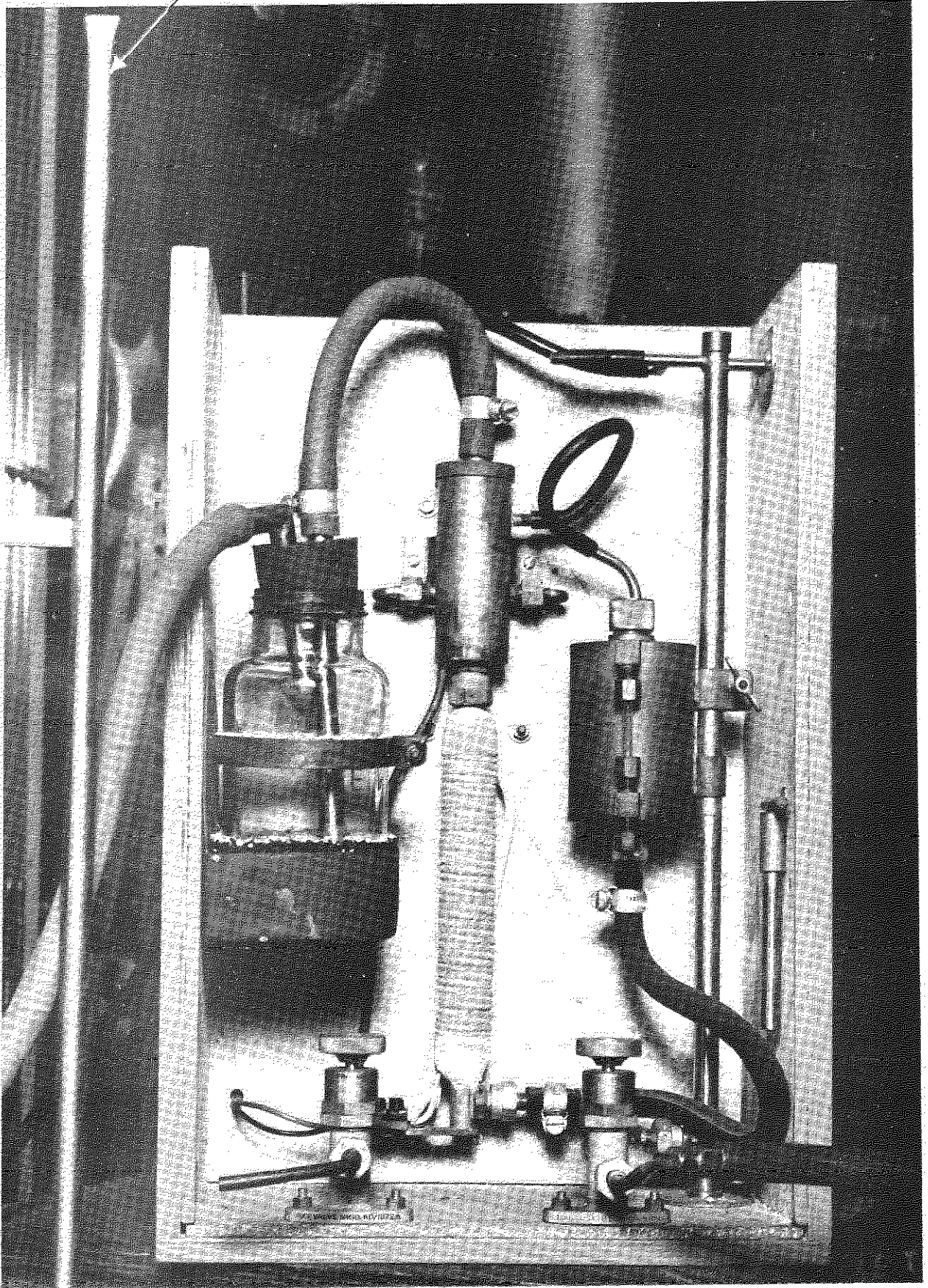
SMOKE GENERATOR WITH SMOKE PROBE.

FIG. 9

MEAN MIXING LINE

b DEPTH OF MIXING REGION
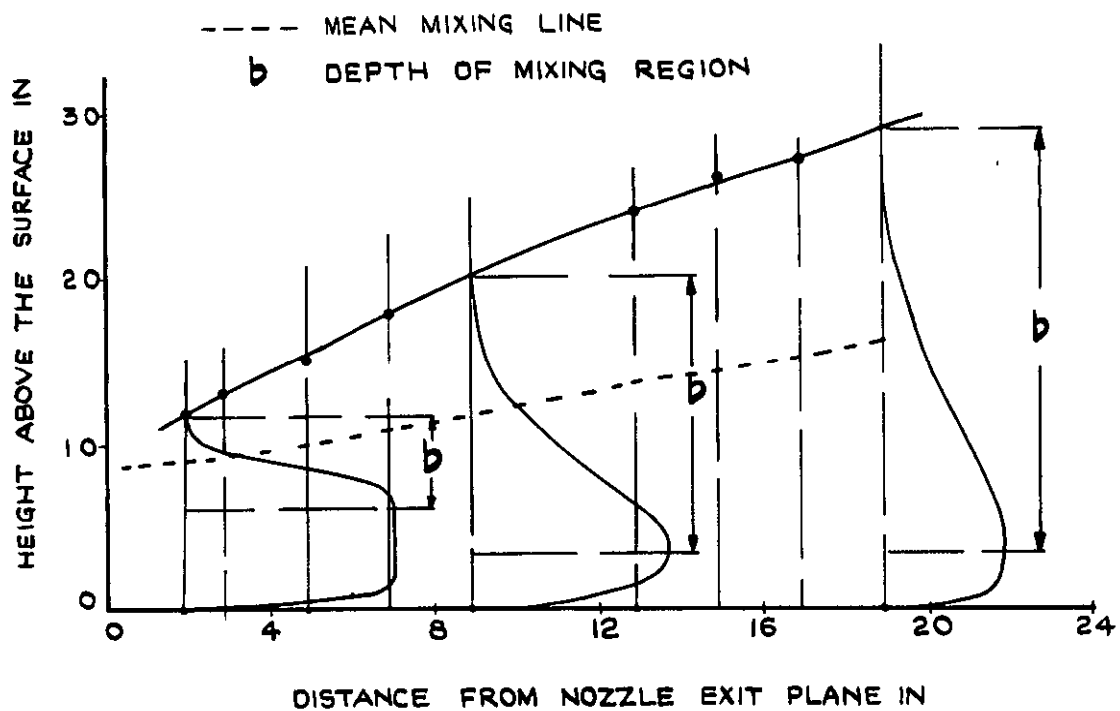
FIG 9a. DETERMINATION OF THE MEAN MIXING LINE.
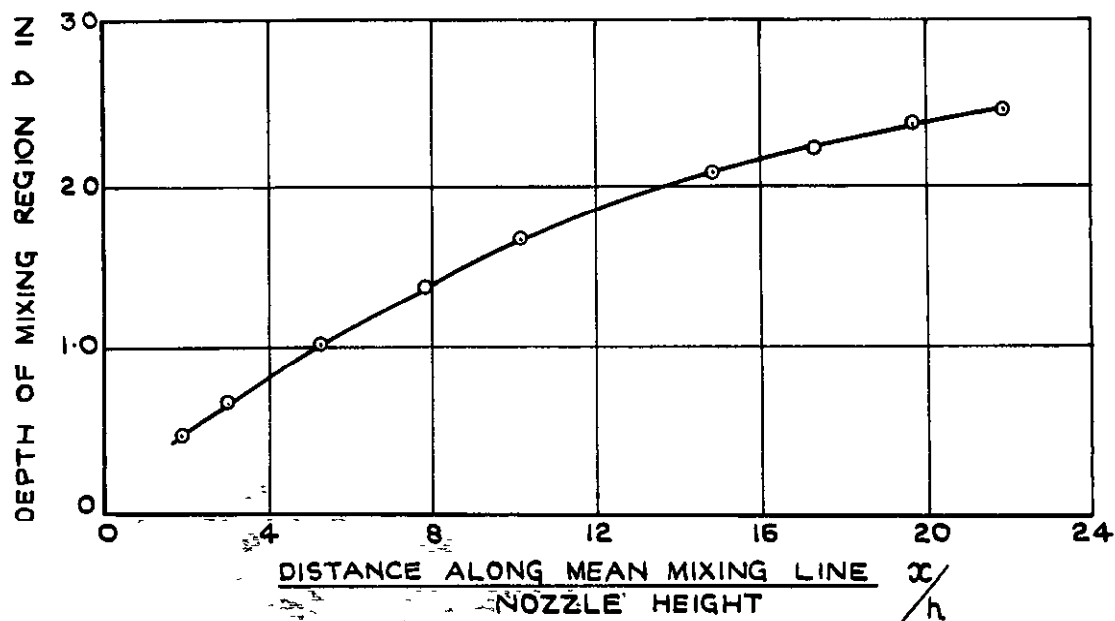
FIG.9b. VARIATION OF THE DEPTH OF MIXING REGION WITH x/h.

24 IN. STRAIGHT MODEL —
ANALYSIS BASED ON PRESSURE TRAVERSES
INSIDE THE JET STREAM.
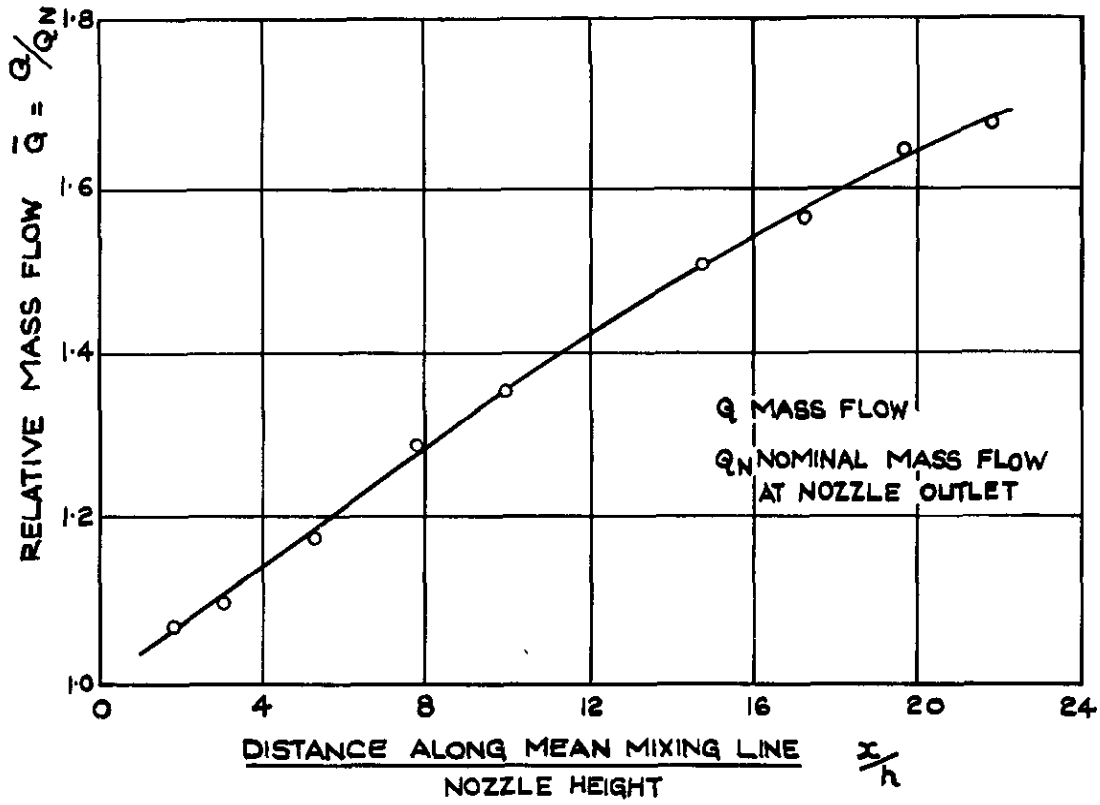
FIG IO a. VARIATION OF RELATIVE MASS FLOW WITH x/h.
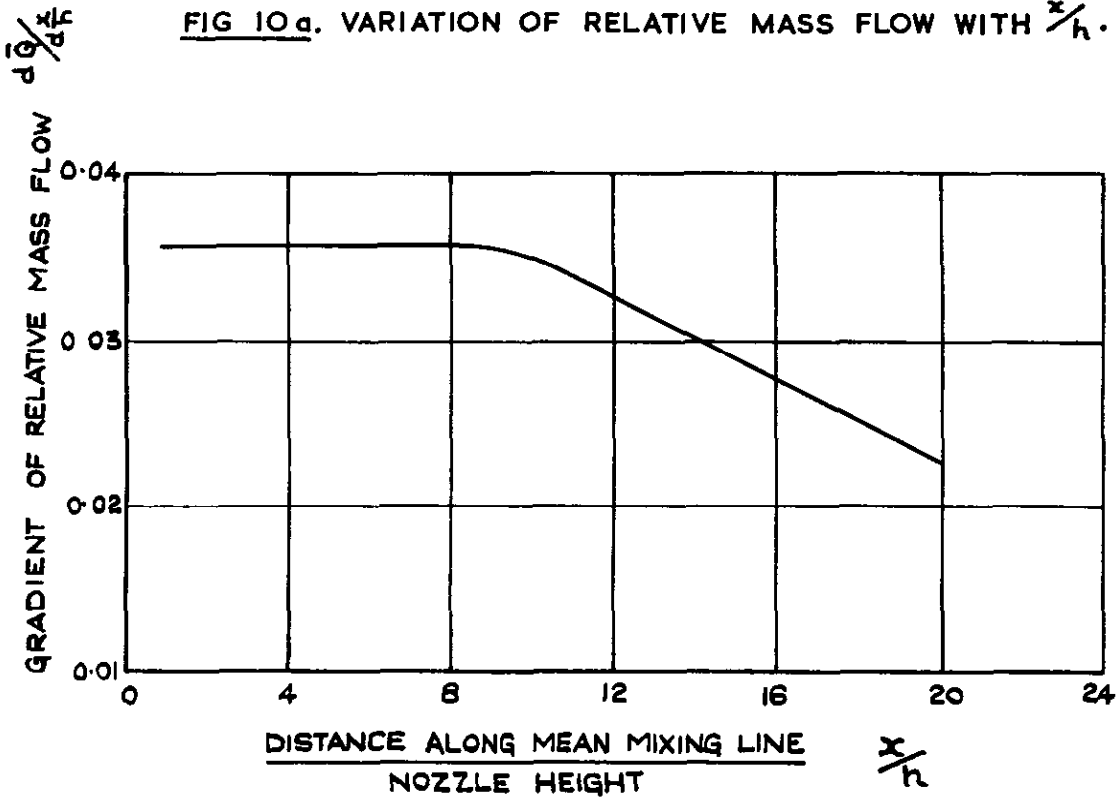
FIG. IO b. VARIATION OF GRADIENT OF RELATIVE MASS FLOW WITH x/h.

24 IN. STRAIGHT MODEL – ANALYSIS BASED ON PRESSURE TRAVERSES INSIDE THE JET STREAM.

FIG.II
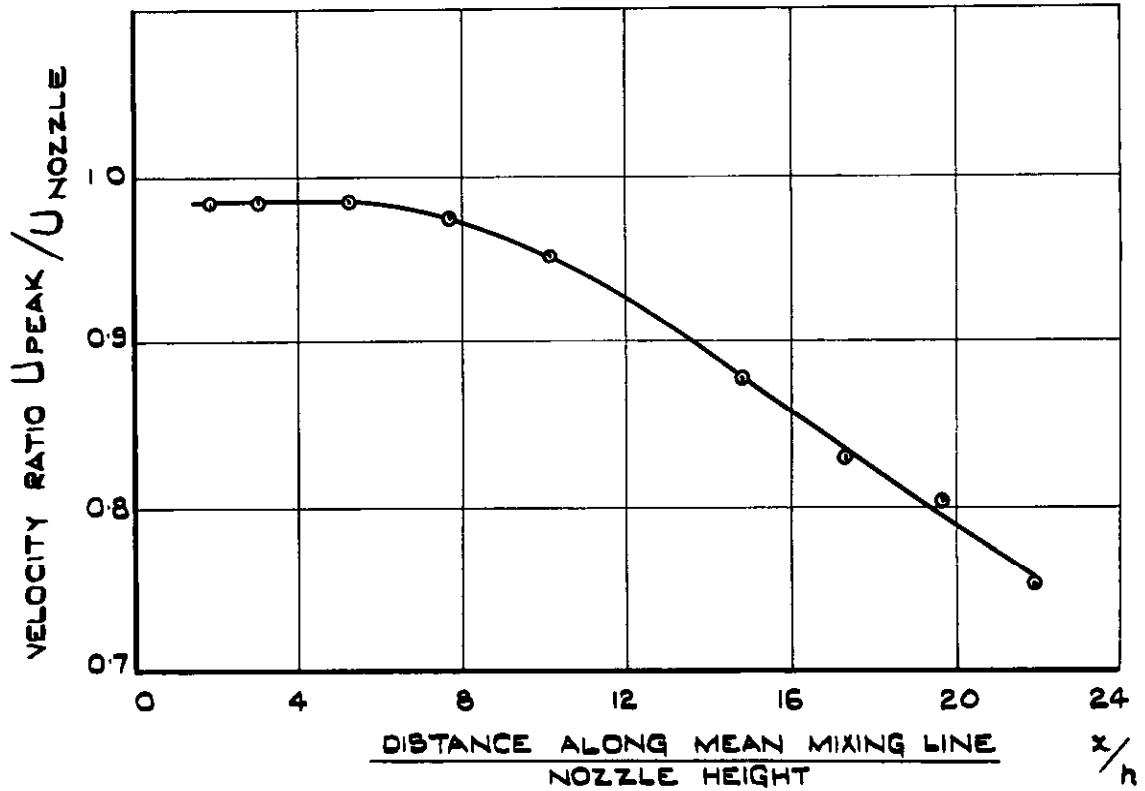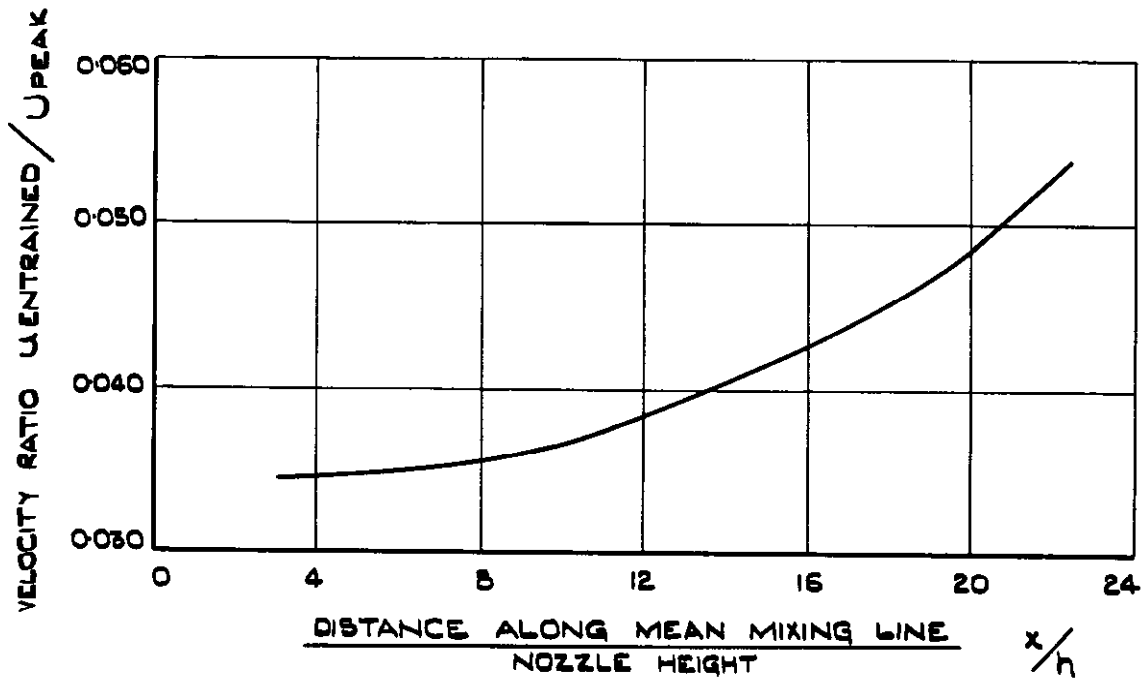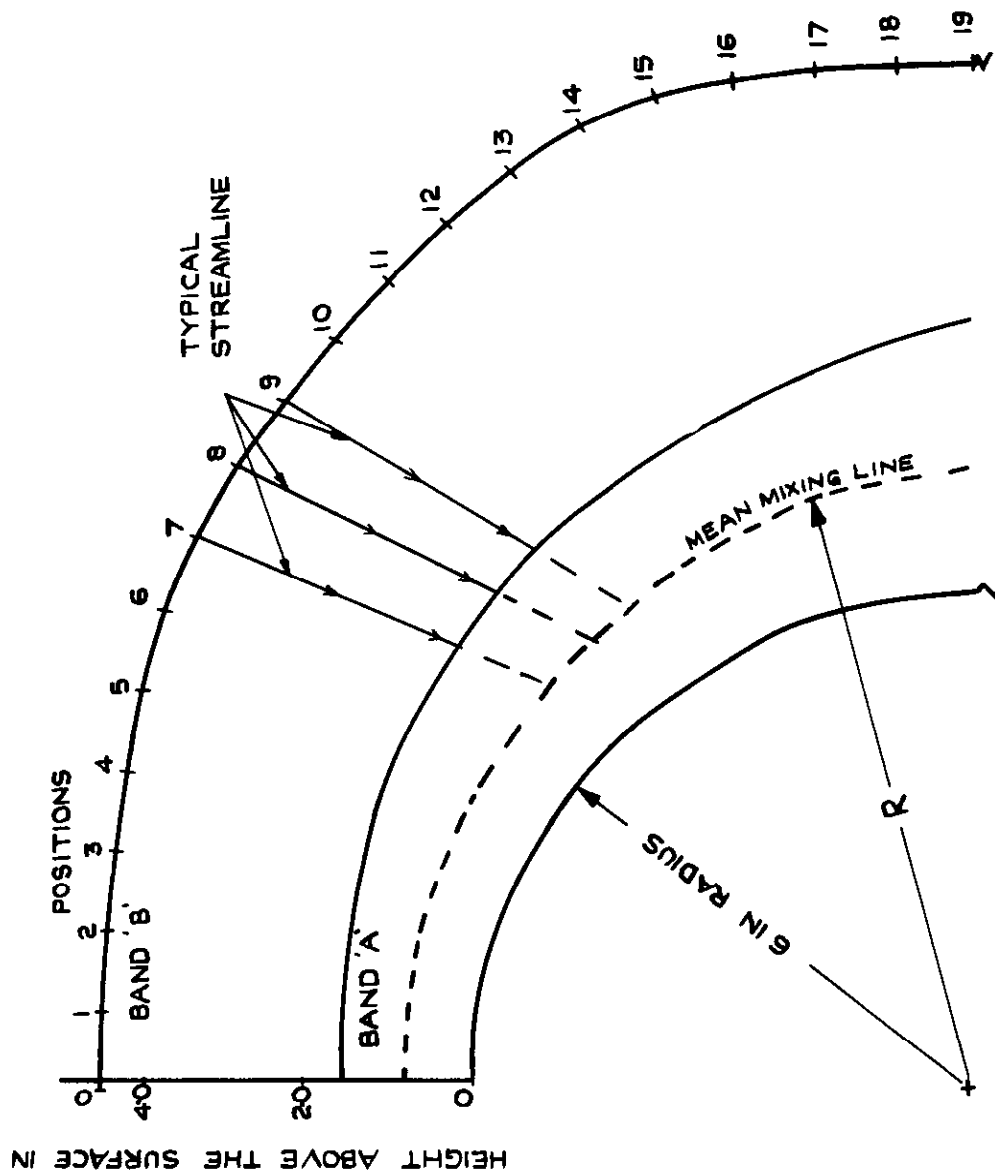

FIG IIa. VARIATION OF VELOCITY RATIO U_{PEAK}/U_{NOZZLE} WITH x/h.
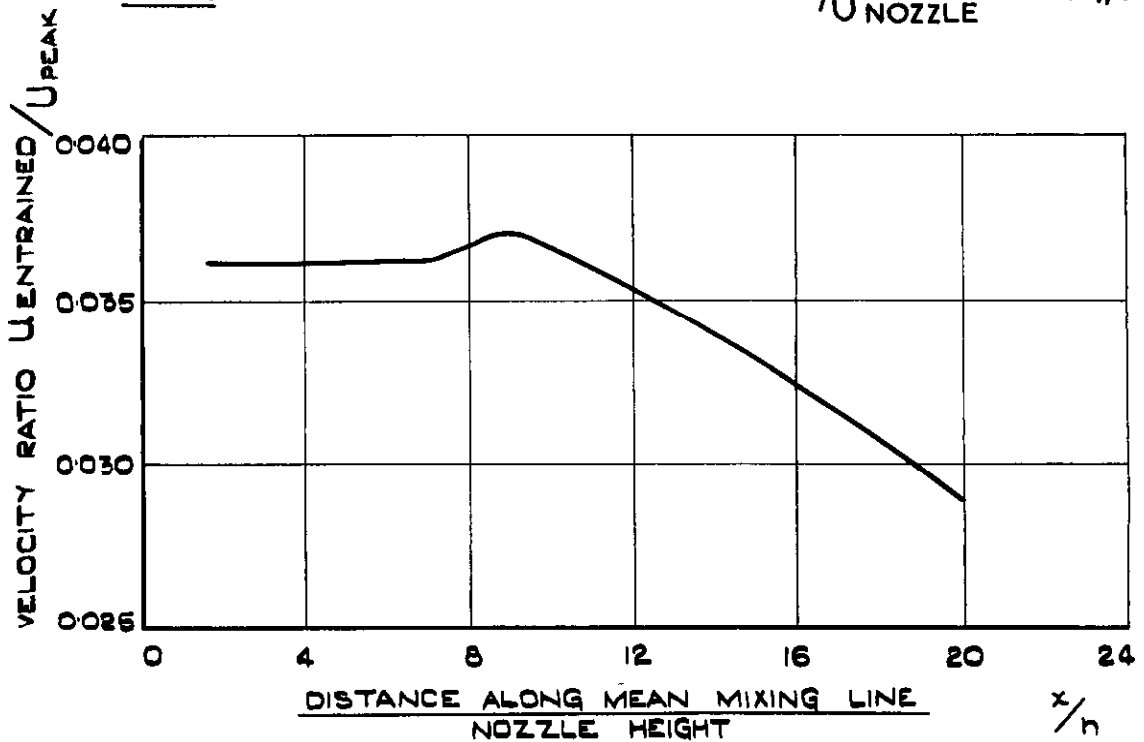
FIG IIb. VARIATION OF VELOCITY RATIO $U_{ENTRAINED}/U_{PEAK}$ WITH x/h.

24IN. STRAIGHT MODEL — ANALYSIS BASED
ON PRESSURE TRAVERSES INSIDE THE JET STREAM.

FIG. 12
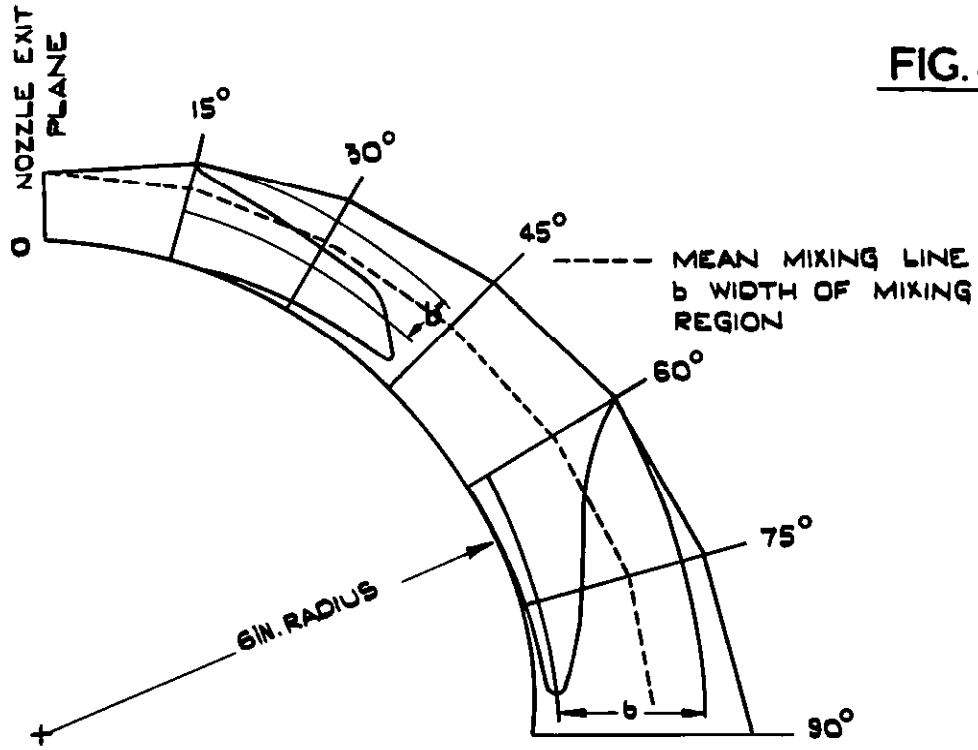
FIG 12a. DETERMINATION OF THE MEAN MIXING LINE
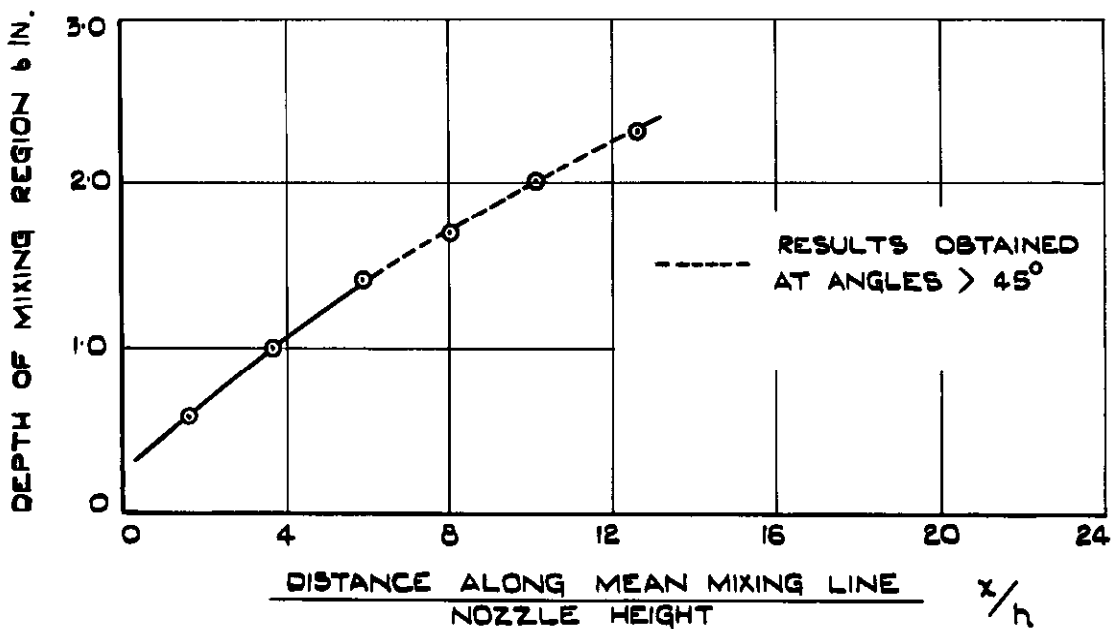
FIG.12b. VARIATION OF THE DEPTH OF THE MIXING REGION WITH x/h.

6IN. RADIUS MODEL—ANALYSIS BASED ON
PRESSURE TRAVERSES INSIDE THE JET STREAM.

FIG. 13
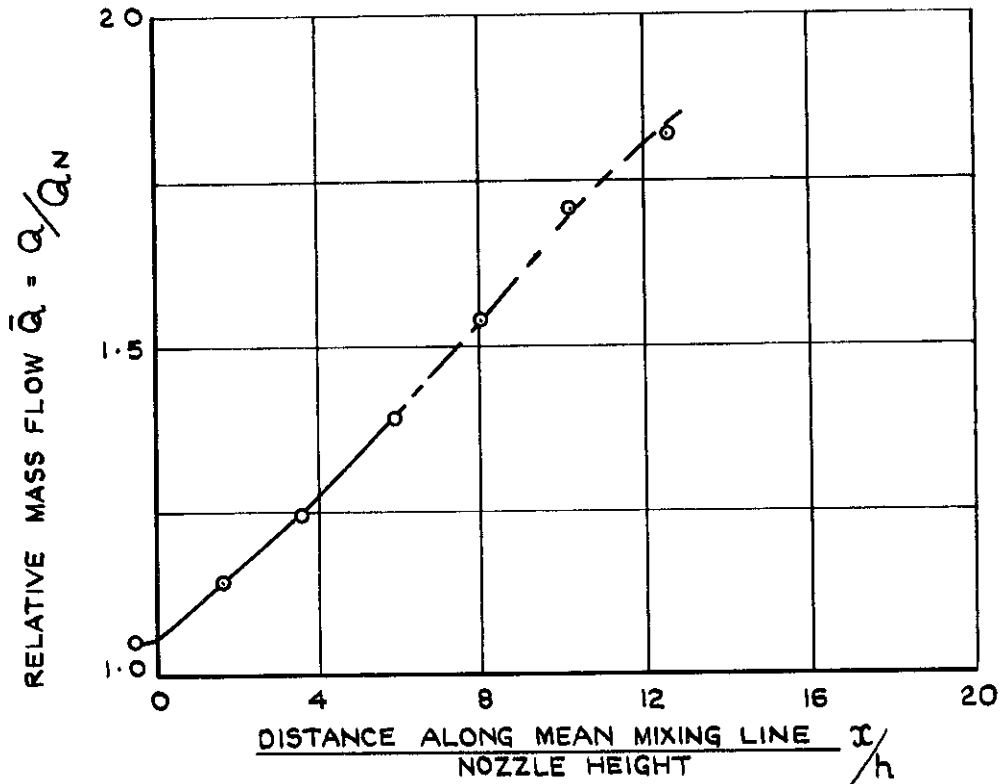
FIG 13 a. VARIATION OF RELATIVE MASS FLOW WITH x/h.
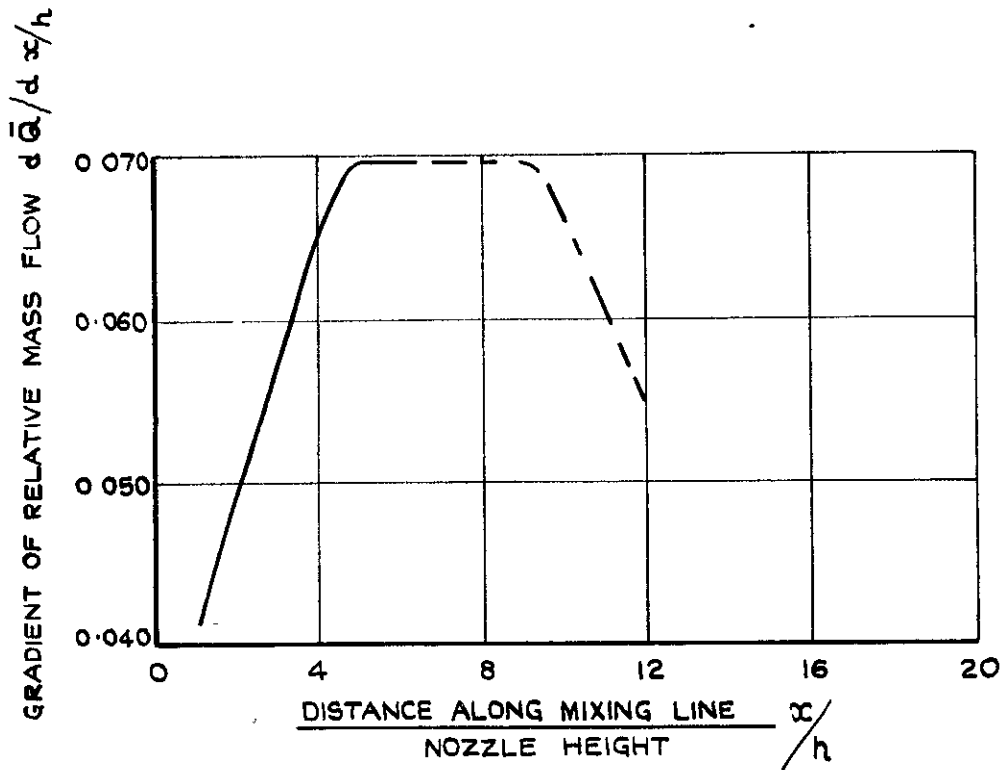
FIG 13 b VARIATION OF THE GRADIENT OF RELATIVE MASS FLOW WITH x/h.

6 IN. RADIUS MODEL —
ANALYSIS BASED ON PRESSURE TRAVERSES
INSIDE THE JET STREAM.

FIG. 14
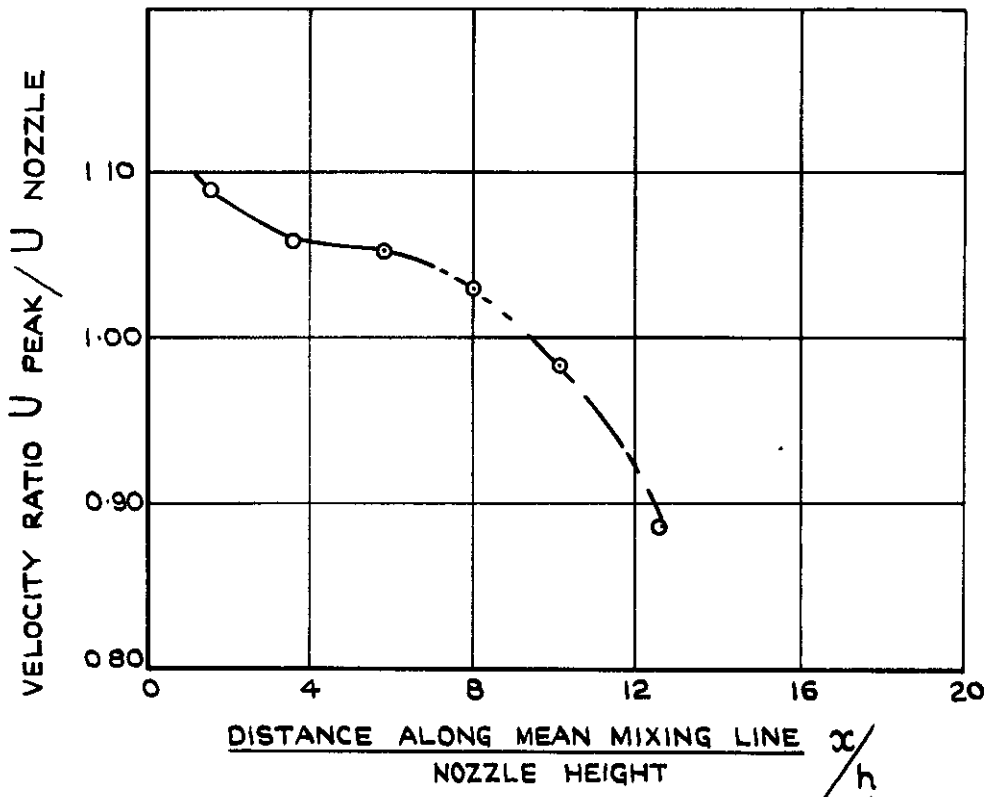
FIG.14a. VARIATION OF VELOCITY RATIO U PEAK$/U$ NOZZLE WITH $^x/_h$.
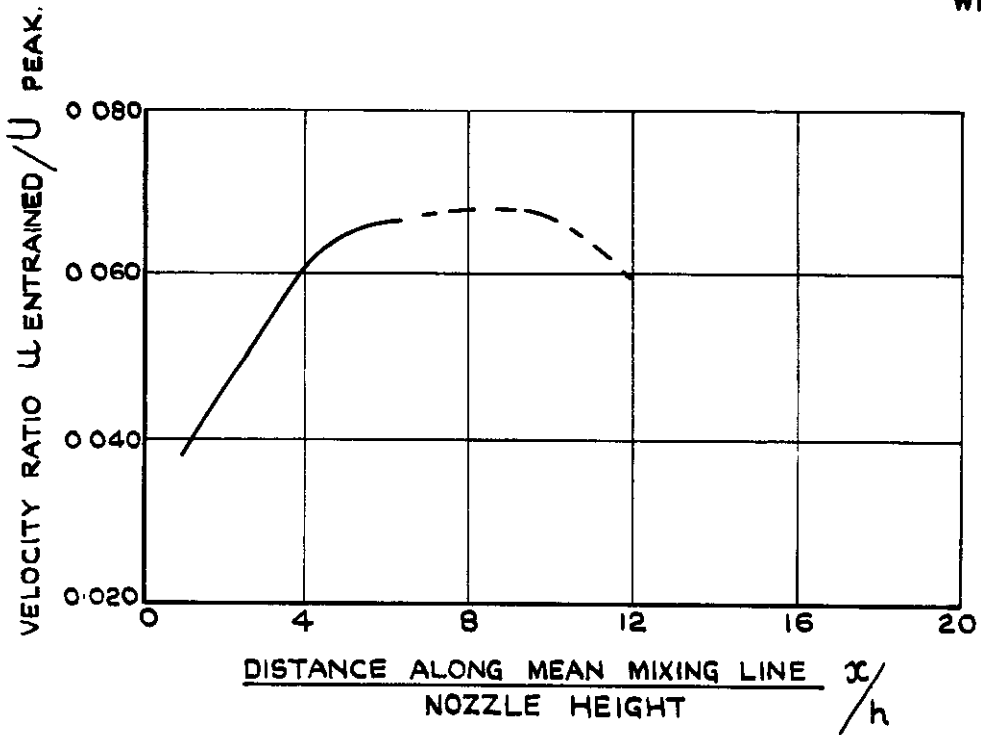
FIG.14b. VARIATION OF VELOCITY RATIO UENTRAINED$/U$PEAK WITH $^x/_h$.

6 IN. RADIUS MODEL —
ANALYSIS BASED ON PRESSURE TRAVERSES
INSIDE THE JET STREAM.

FIG. 15

	RESULTS FROM MASS FLOW ANALYSIS	RESULTS FROM DIRECT ENTRAINMENT VELOCITY ANALYSIS
4 IN RAD. 24 IN STR	—— · —— ·	—— · · —— ·
6 IN RAD 24 IN STR	— — · — —	— — · · — — · ·
6 IN STR 4 IN RAD 24 IN STR	—— ——	— — — —
6 IN STR 6 IN. RAD 24 IN STR	— — — —	— — — ——
THEORETICAL LINE	——————	
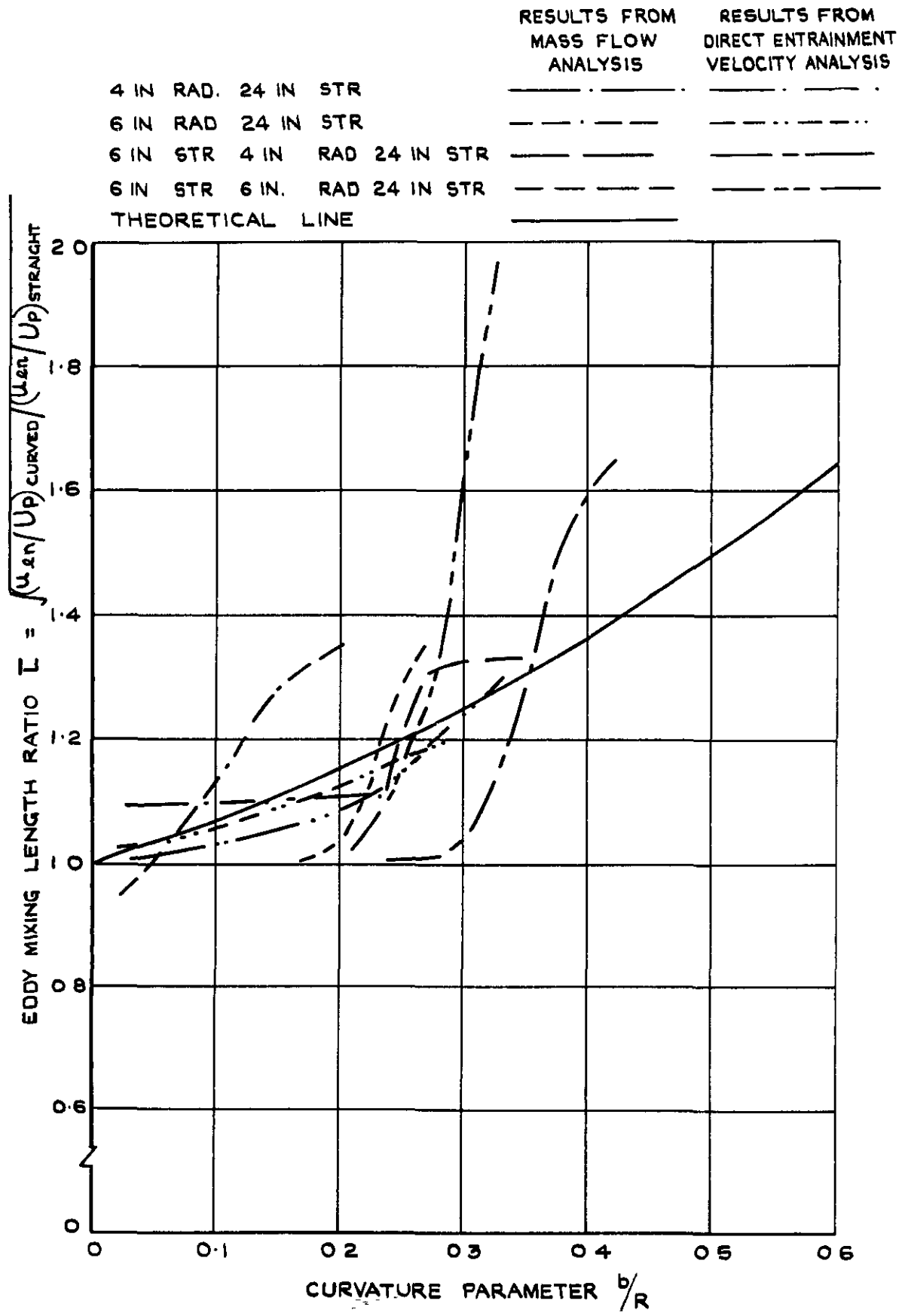
EXPERIMENTAL RESULTS —
RATIO $\overline{L}$ OF EDDY MIXING LENGTH
IN CURVED AND STRAIGHT FLOWS.
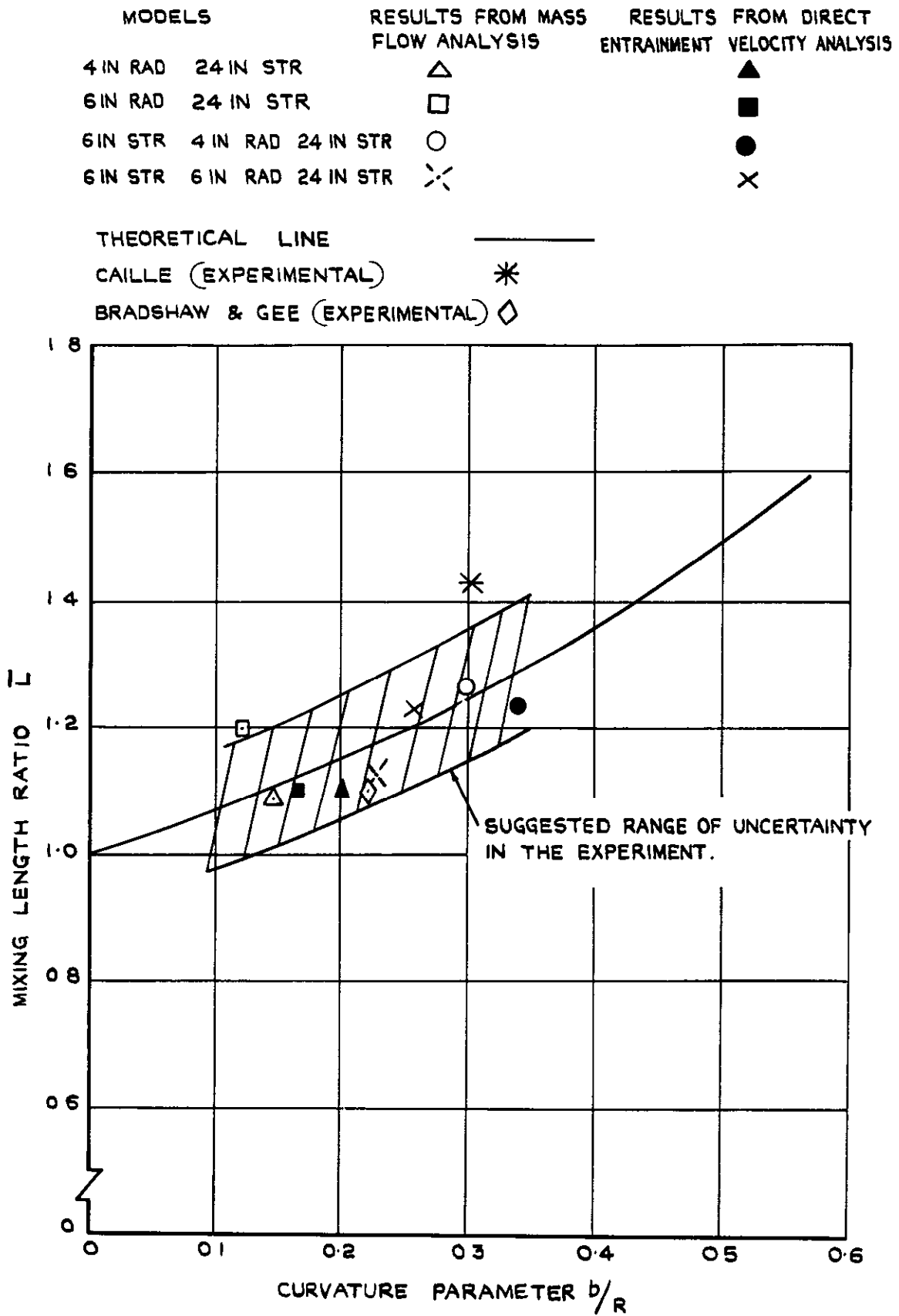
EXPERIMENTAL RESULTS BASED ON MEAN VALUES-
RATIO $\overline{L}$ OF EDDY MIXING LENGTH IN CURVED
AND STRAIGHT FLOWS.
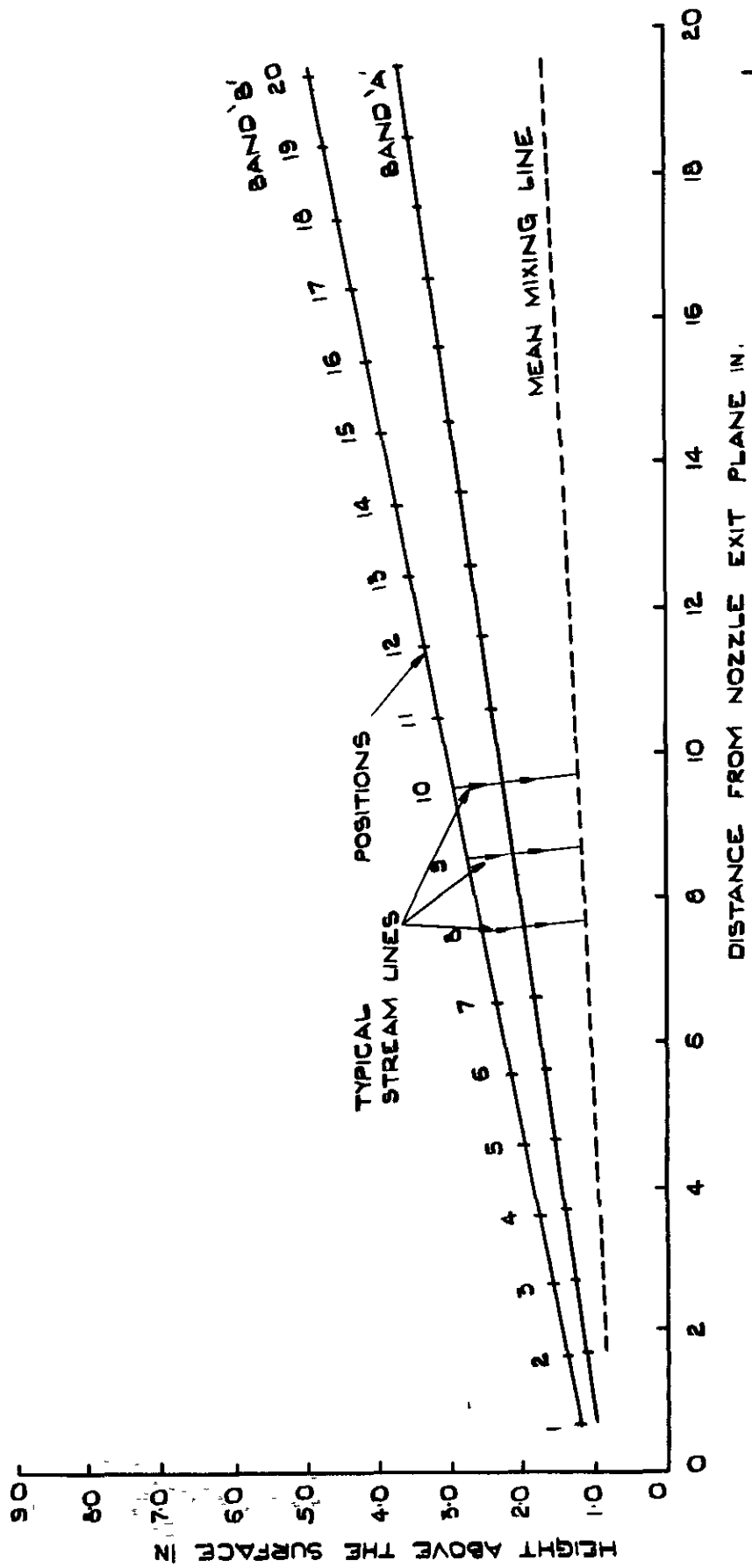
FIG.17

24IN STRAIGHT MODEL—ANALYSIS BASED ON
DIRECT MEASUREMENT OF ENTRAINED VELOCITY.
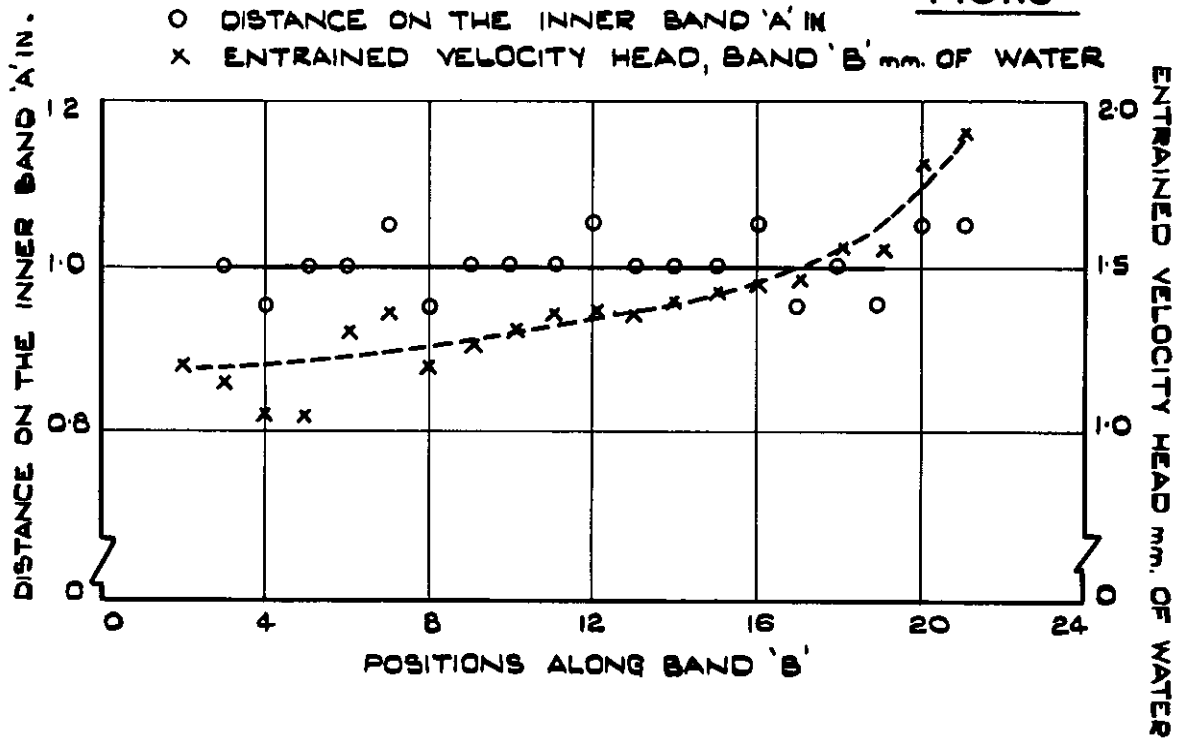
FIG.18

FIG.18 a. DISTANCE BETWEEN NEIGHBOURING STREAMLINES ON
BAND 'A'; ENTRAINED VELOCITY HEAD ON BAND 'B'.

FIG.18b. VARIATION OF VELOCITY RATIO $U_{ENTRAINED}/U_{PEAK}$ WITH x/h.

24IN STRAIGHT MODEL—ANALYSIS BASED ON
DIRECT MEASUREMENT OF ENTRAINED VELOCITY.

FIG. 19

6 IN. RADIUS MODEL — ANALYSIS
BASED ON DIRECT MEASUREMENT OF
ENTRAINED VELOCITY.

FIG. 20
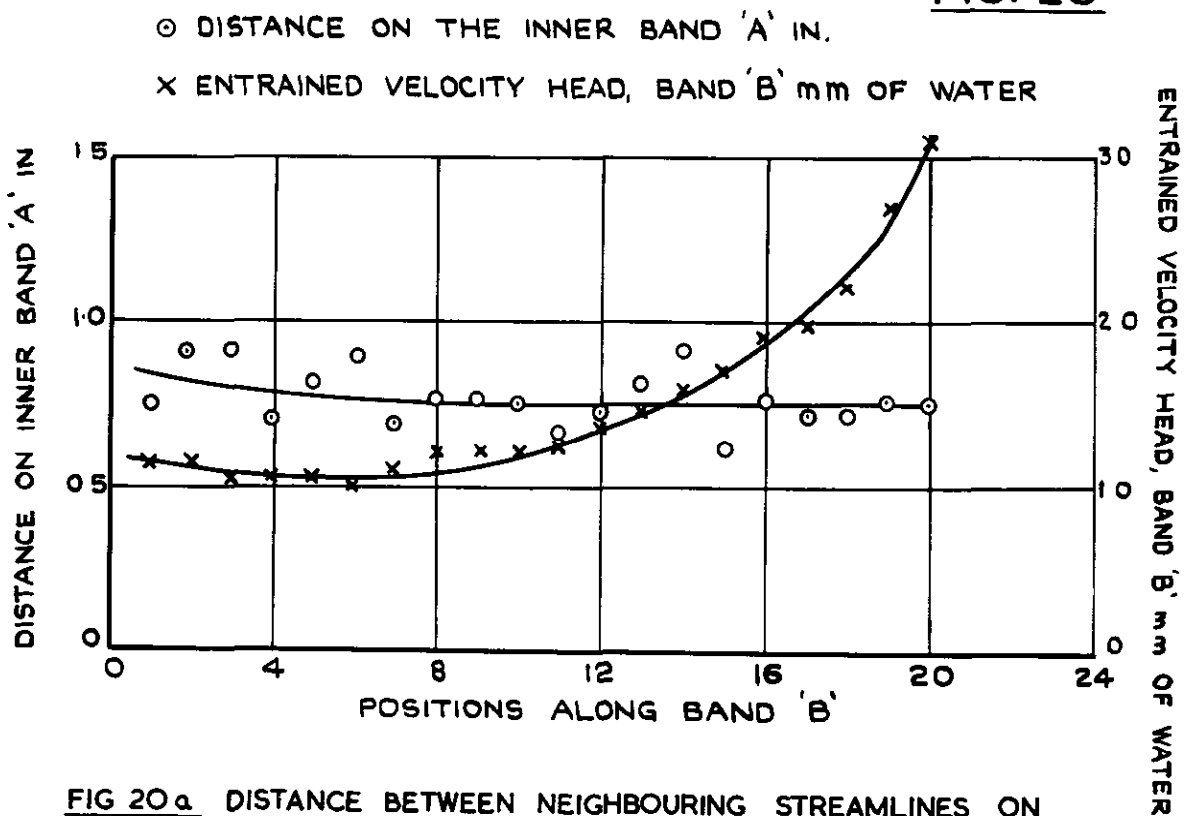
⊙ DISTANCE ON THE INNER BAND 'A' IN.

✕ ENTRAINED VELOCITY HEAD, BAND 'B' mm OF WATER

FIG 20a DISTANCE BETWEEN NEIGHBOURING STREAMLINES ON
BAND 'A', ENTRAINED VELOCITY HEAD ON BAND 'B'.

— — RESULTS OBTAINED AT
ANGLES ⟩ 75°
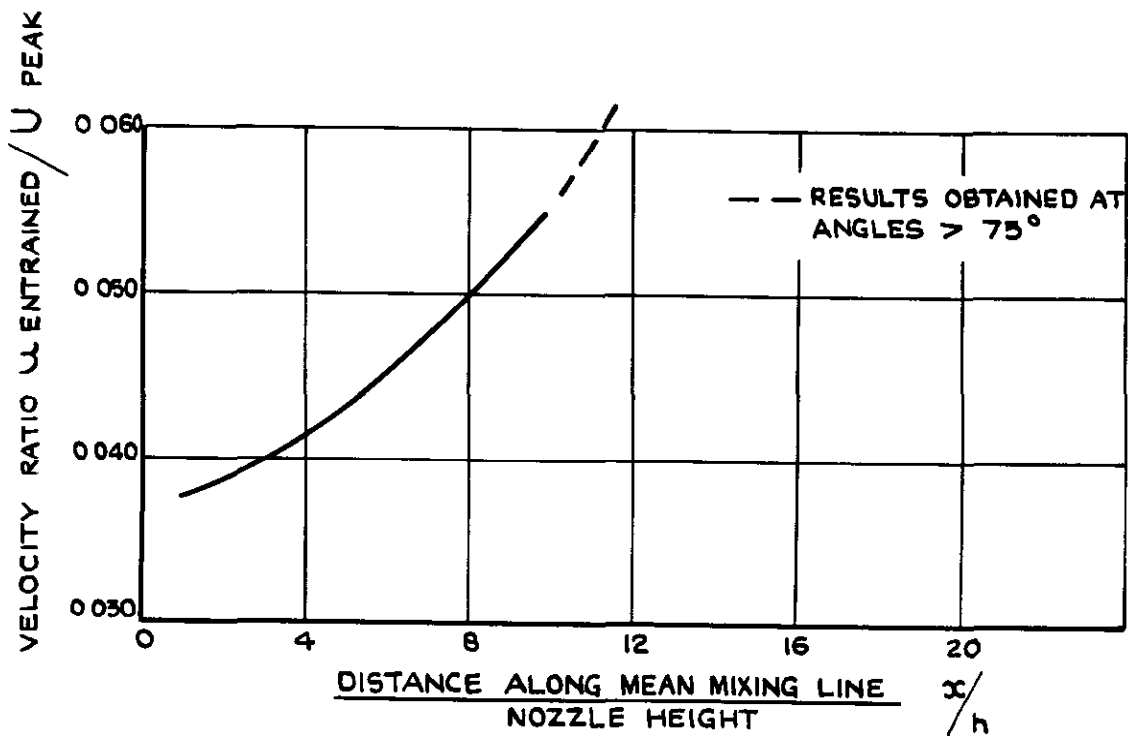
FIG. 20b. VARIATION OF VELOCITY RATIO U ENTRAINED/U PEAK WITH x/h.

6 IN. RADIUS MODEL — ANALYSIS
BASED ON DIRECT MEASUREMENT OF
ENTRAINED VELOCITY.

A.R.C. C.P. No. 687, June 1962.   532.529.3
Stratford, B. S., Jawor, Z. M. and Golesworthy, G. T.
        THE MIXING WITH AMBIENT AIR OF A COLD AIRSTREAM
                  IN A CENTRIFUGAL FIELD

   Tests have been made to compare the rate of mixing with
ambient air of a single-sided cold air jet when flowing
over straight and curved surfaces. The rate of mixing,
defined as the rate of entrainment of ambient air into
the stream, was determined in two ways: from direct
measurement of the increase of mass flow inside the jet
and from the entrainment velocity derived from measure-
ments of the static pressure close to the jet boundary.

   The experimental results, though showing consid-
erable scatter, lend confirmation to earlier deductions
that a centrifugal field increases the mixing rate. A
typical increase in mixing rate is 50%.

A theoretical analysis, developed from mixing
length concepts, shows that the increase in mixing rate
is approximately proportional to the strength of the cen-
trifugal field. The increase results from the eddies of
air from the higher momentum stream being centrifugal
through surrounding air of lower momentum.

The experimental results are broadly in agreement
with the theory, as well as with previous experimental
work.

A theoretical analysis, developed from mixing
length concepts, shows that the increase in mixing rate
is approximately proportional to the strength of the cen-
trifugal field. The increase results from the eddies of
air from the higher momentum stream being centrifugal
through surrounding air of lower momentum.

The experimental results are broadly in agreement
with the theory, as well as with previous experimental
work.

A theoretical analysis, developed from mixing
length concepts, shows that the increase in mixing rate
is approximately proportional to the strength of the cen-
trifugal field. The increase results from the eddies of
air from the higher momentum stream being centrifugal
through surrounding air of lower momentum.

The experimental results are broadly in agreement
with the theory, as well as with previous experimental
work.

A theoretical analysis, developed from mixing
length concepts, shows that the increase in mixing rate
is approximately proportional the the strength of the cen-
trifugal field. The increase results from the eddies of
air from the higher momentum stream being centrifugal
through surrounding air of lower momentum.

The experimental results are broadly in agreement
with the theory, as well as with previous experimental
work.